Winter 2004

Inter-Annual to Inter-Decadal Variability of Upwelling and Anchovy Population off Northern Chile

Jose L. Blanco-Garcia
Old Dominion University

INTER-ANNUAL TO INTER-DECADAL VARIABILITY OF UPWELLING AND ANCHOVY POPULATION OFF NORTHERN CHILE

by

Jose L. Blanco-Garcia
Physical Oceanographer - Universidad Católica de Valparaíso (1984)

A Dissertation submitted to the Faculty
of Old Dominion University in Partial Fulfillment of the
Requirement for the Degree of

DOCTOR OF PHILOSOPHY

OCEANOGRAPHY

OLD DOMINION UNIVERSITY
December 2004

Approved by:

_____
Larry P. Atkinson (Director)

_____
Chester E. Grosch (Member)

Thomas C. Royer (Member)

Franklin B. Schwing (Member)

ABSTRACT

INTER-ANNUAL TO INTER-DECADAL VARIABILITY OF UPWELLING AND ANCHOVY POPULATION OFF NORTHERN CHILE

Jose L. Blanco-Garcia
Old Dominion University, 2004
Director: Dr. Larry P. Atkinson

The coastal ocean of northern Chile has persistent wind-driven upwelling that produces high nutrient and chlorophyll concentrations in a narrow band along the coast. The objective of this thesis is to study the low frequency temporal variability of the upwelling system, to understand the spatial and temporal changes in the wind field, and how these changes may affect the upwelling and anchovy variability. Data used in this thesis includes time series of wind, sea level, sea surface temperature, and atmospheric pressure at coastal stations, from 1960 to 2003, and oceanographic and acoustic cruises for the period 1993-2003. The time series are analyzed using the STL method (Seasonal Trend Decomposition procedures based on locally weighted regression and smoothed scatter plots (LOESS)), maxima entropy spectral analysis, wavelets, cross spectra, and EOFs (Empirical Orthogonal functions). The wind field from ERS and QuikSCAT satellite radar scatterometers was analyzed.

Variability occurred at four frequency bands: quasi-biennial (2-3 years), ENSO (3-8 years), decadal (9-12 years), and interdecadal (13-25 years). The origin of quasi-biennial variability could be explained by means of the Delayed Oscillator Mode. The STL trend shows three regime changes: before 1976 (cold), between 1976 and 1998 (warm), and after 1998 (cold). These regime changes correspond with the changes in anchovy and sardine populations in the Chile-Peru system. During the last five years, there has been a diminution of the upwelling index, SST, sea level, and atmospheric pressure, and more Lasker events (calms).

The spatial variability of wind stress in the study area is characterized by a minimum between two maximums located at 15°S and 30°S. The effect of the curvature of the coast, as well as the height of mountains near the coast, produces a unique system, where the wind is forced thermally, reaching a maximum in summer and a minimum in winter, in opposition to the oceanic pattern. In spring and summer the alongshore wind is accelerated by cross-shore pressure gradient changes, producing an intense divergence along the coast. Very near the coast, the wind stress is low, though it increases offshore. The combined effect of both processes produces a convergence outside of the upwelling front. On the scale of days, this convergence could be the

origin of the mesoscale eddies that are observed in the zone. This pattern changes during ENSO events.

El Niño produced changes in the density, distribution, and the depth of the anchovy schools. The deepening of some schools in the coastal area placed them below normal fishing nets, explaining their fast recovery when the El Niño ends.

With love to my wife Ivonne, and my children Beatriz and Jose Luis.

To the memory of my mother, Maria Garcia. She woke-up my love for adventure.

ACKNOWLEDGMENTS

I would like to acknowledge to the following people: my family and friends who always supported me and who made this experience one of the most important in my life; to Dr. Arnoldo Valle-Levinson, who helped me and facilitated my decision of to come here; to Dr. Larry Atkinson who believed, encouraged, and supported me constantly; and to all the teachers that I had the luck to know, whose classes I learned and enjoyed. I am also thankful to the faculty and staff members for their support and help. To all the colleagues and friends who helped me obtain the necessary information to develop the thesis. To the Instituto de Fomento Pesquero de Chile (IFOP) for providing the oceanographic cruise data, which was funded by the Fondo de Investigacion Pesquera (FIP projects from 1993 to 2003). To the Servicio Hidrografico y Oceanografico de la Armada de Chile (SHOA) and the Direccion Meteorologica de Chile for providing time series information.

TABLE OF CONTENTS

LIST OF TABLES

LIST OF FIGURES

INTRODUCTION

The coastal ocean of northern Chile is part of the Humboldt Current System. The region has persistent wind-driven upwelling during most of the year, with maximum upwelling in summer and weakest upwelling in winter (Strub et al., 1998; Blanco et al., 2001). The mean conditions, based on 30 years of data, along with a description of the most important processes and the characterization of the water masses were described by Blanco et al. (2001). This region presents significant interannual variability with the most relevant periodicity related to the El Niño Southern Oscillation (ENSO) cycle (Wyrtki, 1976; Blanco et al., 2002).

The study area (Fig. 1) is located where the coast of South America changes from a north-south orientation to a northwest-southeast orientation at 18°S. The mountains close to the coast reach over 3,000 m and the continental shelf is very narrow and practically non-existent. In the nearby Pacific trench depths reach >6000 m.

The upwelling process results in a system of high nutrient and resultant high chlorophyll concentrations that causes a high biomass and species richness in this area that supports important benthic, demersal, and pelagic fisheries. Anchovy and sardine are the dominant pelagic fish species and they alternate in predominance on a decadal time scale (Fig. 2) (Schwartzlose et al., 1999; Alheit & Niquen, 2004).

A major issue is how to link this climatic variability to the biological populations involved. It has been suggested that three classes of processes tend to determine favorable reproductive habitats for fish stocks (Bakun, 1996; Schwartzlose et al., 1999): enrichment processes (upwelling, mixing, Ekman divergence and cyclonic eddy formation), concentration processes (convergent frontal formation, Ekman convergence, and lack of dispersion by turbulent mixing processes (Lasker's stability hypothesis)), and retention processes (lack of offshore transport in Ekman field, availability of enclosed gyral circulations, and stability of current patterns to which life cycles are adapted). Beside these processes, food availability and temperature have been thought also to be key factors (Schwartzlose et al., 1999; Alheit & Niquen, 2004).

Considering the mentioned variations of the environment regimes and the resultant effect on the pelagic fish, the following questions must be asked:

1- When was the last regime shift?

2- What is the origin of the quasi-biannual variability?

3- How is upwelling affected by ENSO and decadal cycles?

The Journal *Progress in Oceanography* was used as the Journal model

4- What is the spatial variability of the wind field and how does it relate to the observed biological variability?

5- Does the wind measured at coastal stations represent the offshore wind field?

6- Is the satellite wind data useful for studies of processes in the area?

7- What is the importance and magnitude of cross and alongshore transport?

8- What are the mechanisms for larval dispersion, retention, and variability?

This thesis attempts to answer questions 1 to 6 and discusses some ideas relevant to questions 7 and 8, filling a significant gap in the knowledge of the low frequency coastal - ocean dynamic processes and their effect on the pelagic fish population in northern Chile (18° - 24°S).

The specific objectives of this research are:

1. To determine the low frequency variability of the principal variables, and if they are affected by local or remote processes.
2. To characterize the wind field in the area, and the effects on physical, chemical and biological processes.
3. To describe the response of anchovy populations to environmental changes.

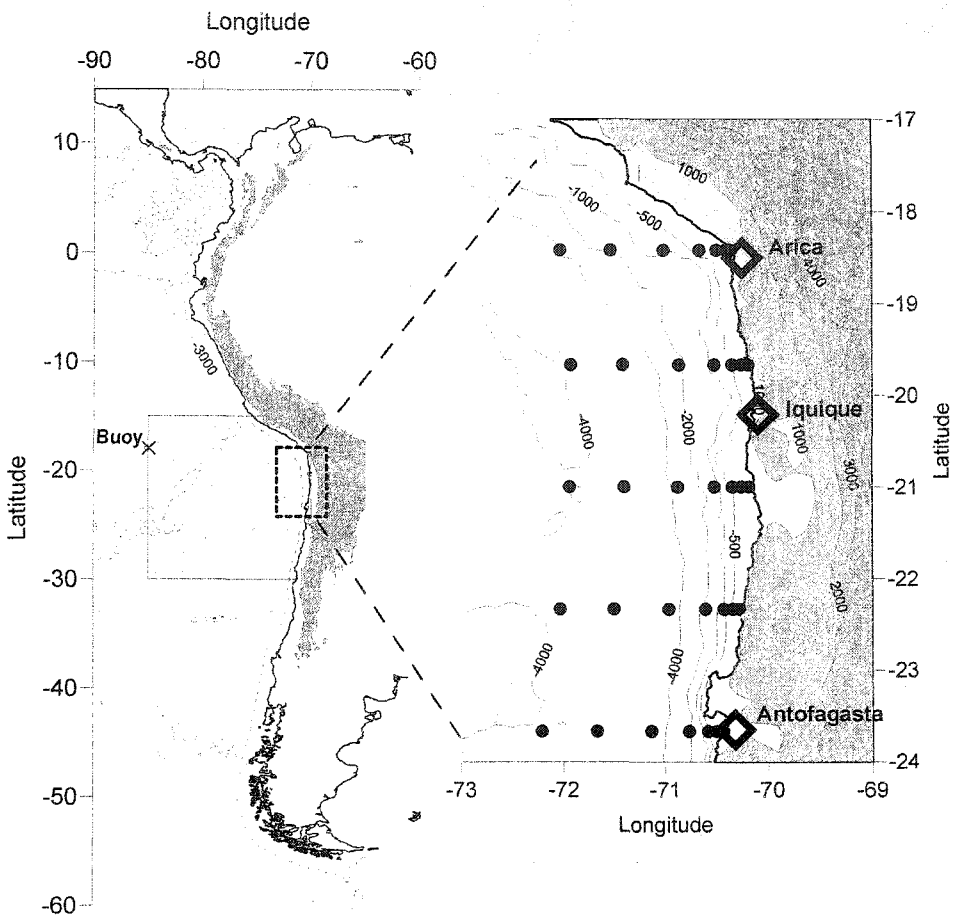

Fig. 1. Left map: Study area (segmented line in the shaded box) and satellite wind data (shaded box, solid line), the symbol x correspond to the position of the TOGA-TAO buoy #32302, dark area in the continent show the mountains elevation (> 2000 m). Right map: magnification of study area, showing coastal stations (diamond), oceanographic stations for the seasonal cruises (circle), bathymetry, and mountains elevation.

BACKGROUND

Physical oceanographic variables have been clearly linked with oceanic ecosystem changes at many temporal and spatial scales. Physical forcing is especially obvious in seasonal (and shorter) time scales where variations in sea-surface temperature (SST) and upwelling, for example, strongly influence productivity, growth and migration patterns. This forcing is also evident in interannual timescales associated with ENSO events (El Niño and La Niña episodes), when the Southeastern Pacific is remotely forced by oceanic and atmospheric teleconnections.

In the North Pacific Ocean, patterns of low-frequency variability in the climate and ecological systems have been referred to as the "Pacific (inter) Decadal Oscillation" or PDO (Mantua et al., 1997), the "Inter-decadal Pacific Oscillation" or IPO (Power et al., 1999), the Pacific "Decadal and Interdecadal Climatic Event" or DICE (Nakamura and Yamagata, 1997) or the "Bi-Decadal Oscillation' or BDO (Cook et al., 1997). Also, Torrence and Webster (1999) and White et al. (2003) present evidence that low-frequency climate fluctuations modulate El Niño intensity.

Physical forcing processes that affect oceanic ecosystems range from those associated with the smallest scales of dissipation, turbulent mixing, and diffusion; to those acting on the mesoscale associated with fronts, eddies, and upwelling; to those operating on the basin scale associated with gyres, El Niño, and the thermohaline circulation (Denman et al., 1996). The regional and local manifestations of this physical forcing on the biology can occur instantaneously or with a time delay.

Sea surface temperature (SST), mixed-layer depth (MLD), thermocline depth, upwelling strength, and upper-ocean current fields are among the most important of the physical oceanographic variables that can influence marine populations. Correlations between these physical variables and long-term changes in ecosystems have routinely been identified, but the specific mechanisms involved are usually difficult to elucidate. The challenge is to understand the mechanisms of the responses to these instantaneous and delayed physical environmental changes and the various modes of significant feedback through the trophic web. The basin-scale nature of climate change appears to organize patterns of response in fishery resource populations. In fact, it is known that sardine populations at the basin scale seem to be teleconnected in terms of cycles of high and low abundance, as well as inversely correlated to other fish species such as anchovy and herring (Schwartzlose et al., 1999).

These changes occur with interdecadal periodicity and affect all the physical and biological systems around the world and are known as "Regime shift". According to Mantua

(2004) a Regime shift is "a relatively brief time period in which key state variables of a system are transitioning between different quasi-stable attractors in phase space". Previous regime shifts in 1925, 1950, and 1976 have been mentioned (Chavez et al., 2003). Finally, several authors (Bond et al., 2003; Peterson and Schwing, 2003) show evidence of a recent regime shift in the North Pacific in the late 1990's. Also, this change is mentioned by Chavez et al. (2003) and Alheit and Niquen (2004) as the end of the warm period that started in 1976.

The interannual variability and the El Niño Southern oscillation (ENSO) events have a great influence in the variability of the Humboldt Current System (HCS) (Strub et al., 1998). The ENSO causes important changes in the oceanographic conditions with a significant impact overall marine ecosystem. During El Niño, one of the two extreme states of the ocean–atmosphere system of the Pacific Ocean (Barber, 1988; Philander, 1990), the coasts of Ecuador, Peru, and Chile experience modified circulation patterns and water properties, with increased sea levels and isotherm depths (Strub et al., 1998; Blanco et al., 2002; Carr et al., 2002). Winds usually remain upwelling favorable, but the nutrient supply to the upper layer is generally reduced as upwelled water originates above the deepened nutricline, thus affecting phytoplankton biomass, species composition, and production.

Cold or La Niña periods have received less attention, but they generally lead to shallower nutriclines, which would entail increased nutrient supply, higher phytoplankton biomass, and primary production. These conditions have been recorded in the equatorial Pacific and in the California Current (Murtugudde et al., 1999; Behrenfeld et al., 2001; Hayward et al., 1999; Bograd et al., 2001).

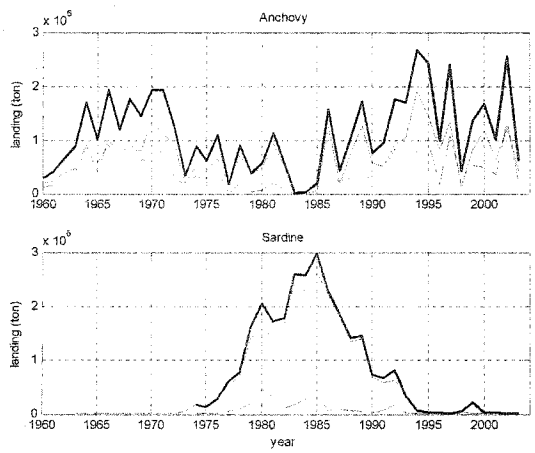

Fig. 2. Anchovy and sardine landing from northern Chile (thin solid line), south of Peru (thin-segmented line), and total (thick line) for the period 1960 – 2002. (Information provided by R. Serra).

METHODS

The study area is the northern part of Chile, from 18.5°S to 24°S and from the coast to 200 km offshore (Fig. 1). In that area there is a good collection of oceanographic data that permits time series statistical analysis. Additionally, there is meteorological, sea level and sea surface temperature from the coastal stations of Arica, Iquique, and Antofagasta (Fig. 2, Table 1) that provide time series longer than 30 years. As complement to the data mentioned in the area, wind data obtained from satellites was analyzed for the area between 15°S to 28°S and 70°S to 85°W (shaded area in Fig. 1) during the period of August 1991 to December 2003.

DATA

Sources of the data are as the follows:

Sea Surface Temperature

Monthly averages of coastal sea surface temperature (SST) were calculated from data measured daily at the coastal stations of Arica (18.5°S), Iquique (20.5°S) and Antofagasta (23.5°S). These data were provided by the Naval Hydrographic Service (Servicio Hidrografico y Oceanografico de la Armada de Chile (SHOA)) for the period 1960-2002.

Sea Level

The coastal sea level (SL) for the coastal station of Callao (12°S) and Antofagasta was obtained from the University of Hawaii Sea Level Center. These data are available for the period 1975 to 2002. Climatological monthly means were calculated after correcting for the inverse barometer effect, Atmospheric pressure data were obtained from the U.S. Climate Analysis Center.

Wind

Monthly averages of wind speed and direction were calculated from daily measurements at the airport meteorological stations of Arica, Iquique, and Antofagasta for the period 1970 to 2003. These data were provided by the Chilean Meteorological Service. The upwelling index (UI) per 1000 m of coast was calculated (Bakun & Parrish, 1982). Additionally, using daily data, the number of Lasker events was determined counting the times when the wind speed is less than 5 m/s for at least 4 days (Lasker, 1978; Peterman & Bradford 1987). This number represents the duration of calm periods or when "the upper mixed layer of the ocean must be in stable

(nonturbulent) state" (Lasker, 1978). Upwelling indices based on estimates of offshore Ekman transport driven by geostrophic wind stress were obtained from the NOAA/NMFS/SWFSC Pacific Fisheries Environmental Laboratory. The data used were from two locations (18°S- 74°W and 21°S-71°W) for the period 1981 to 2001.

Table 1

List of the data from coastal stations, indices, and cruises used in the analysis.

Type	Series	place	Interval	start	end	Source
Coastal Stations						
	SST	Arica	monthly	1970	2003	SHOA
	SST	Iquique	monthly	1976	1999	SHOA
	SST	Antofagasta	monthly	1946	2003	SHOA
	Sea level	Callao	daily	1970	2002	SLC Hawaii
	Sea level	Antofagasta	daily	1946	2003	SLC Hawaii
	Wind	Arica	synoptic	1971	2003	DIMERCHI
	Wind	Iquique	synoptic	1982	2003	DIMERCHI
	Wind	Antofagasta	synoptic	1971	2003	DIMERCHI
	SLP	Antofagasta	monthly	1970	2003	DIMERCHI
	SLP	Easter Island	monthly	1951	2003	DIMERCHI
Indices						
	SOI		monthly	1866	2003	NCEP - NOAA
	OLR		monthly	1979	2003	NCEP - NOAA
	QBO		monthly	1948	2003	CDC - NOAA
	SST	Niño 3.4 & 1+ 2	monthly	1950	2003	NCEP - NOAA
	HCl		monthly	1970	2003	
Cruises						
	t,s,O_2,Chl, z	Arica-Antofagasta	Seasonal	1993	2003	IFOP
	Acoustic	Arica-Antofagasta	Seasonal	1993	2003	IFOP
	Icthyoplancton	Arica-Antofagasta	Seasonal	1993	2003	IFOP
Other information						
	Total anchovy Landing	Arica-Antofagasta	Yearly	1960	2001	IFOP
	Wind satellite	Arica-Antofagasta	weekly	1992	2003	IFREMER

DIMERCHI : Direccion Meteorologica de Chile

SHOA : Servicio Hidrografico y Oceanografico de la Armada de Chile

IFOP : Instituto de Fomento Pesquero

IFREMER : French Research Institute for Exploitation of the Sea

NCEP - NOAA : National Center for Environmental Prediction (NOAA)

t : temperature s : salinity O2 : Oxygen Chl : Chlorophyll z : Depth

Atmospheric pressure

Monthly averages of sea level atmospheric pressure (SLP) obtained in the meteorological stations of Antofagasta and Easter Island (27°9'S, 109°25'W) for the period 1970 to 2003 were provided by the Chilean Meteorological Service.

To analyze the remote forcing in the study area several time series of indexes from outside the study area are used to compare and to estimate the origin of the variability. The series used was the Southern Oscillation Index (SOI), Quasi-Biennial Oscillation index (QBO) and the Outgoing Longwave Radiation (OLR). These data was obtained from the NCEP/NCAR NOAA Reanalysis web page.

Cruise data

Hydrographic and biological information were obtained from oceanographic cruises conducted by the Chilean Fisheries Institute (Instituto de Fomento Pesquero (IFOP)) in the upwelling region off northern Chile (Fig. 1 right). The data used were obtained during the period 1993-2002, but seasonal cruises occurred only from 1996 to present (Table 2).

In each cruise, physical, chemical, and biological data were obtained at 35 oceanographic stations. Temperature and salinity profiles were measured with a standard CTD. Oxygen and chlorophyll *a* were measured from water samples obtained with Niskin bottles at standard depths. Ichthyoplankton was separated and identified from zooplankton net samples; and small pelagic fish school distributions and abundance were determined with acoustic integration.

Table 2

Seasonal cruises used: (o) hydrography, chlorophyll and ichthyoplankton, (+) acoustic

	Summer	Fall	Winter	Spring
1993			o	o
1994	o	o	o +	
1995			o +	
1996	o	o	o	
1997	o	o +	o +	o +
1998	o +	o +	o +	o +
1999	o +	o +	o +	o +
2000	o +	o +	o +	o +
2001	o +	o +	o +	o +
2002	o +	o +	o +	o +
2003	o +	o +	o +	o +

ANALYSIS

The monthly time series were analyzed using two different techniques. The first technique was the traditional: removing the quadratic trend and the monthly mean. The other method to obtain the anomaly was using STL filter (Seasonal-trend decomposition procedures based on LOESS) (Cleveland et al., 1990), which determine the long-term trend and the seasonal variability. The residual (anomaly) values determined by this method improve the variability of the mean, especially when the series has large annual and interannual variability. For the long-term trend a 10 year filter was used. The results obtained by both methodologies (traditional and STL) are compared and discussed.

The anomaly obtained for both methods was smoothed with a fourth order bidirectional Butterworth low-pass filter (Roberts & Roberts, 1978) of 5 months with a half power of 10 months.

The autospectra for each time series was determined using the method of Maxima Entropy (MEM) (Ulrych & Bishop, 1975; Press et al., 1997), where the number of linear predictions was determined as N/2, where N is the length of the time serie (Ghil et al., 2002). The 0.90, 0.95, and 0.99 confidence limits were calculated using the Chi-squared distribution from an autoregressive of second order red spectrum model (AR(2)) as a function of the frequency (f) by the interval (dt) (f*dt) from 0.0 to 0.5 (the Nyquist frequency). The MEM analysis has many advantages over the Fourier spectral analysis, since it allows discrimination in frequency with much better precision.

In addition, a wavelet analysis was carried out to determine time–frequency dominant modes of variability and how they change in time. Wavelet analysis is becoming a common tool for analyzing localized variations of power within a time series (Torrence & Compo, 1998). The wavelet graphics included the cone of influence: a region in which the 'end-effects' due to a finite length of the data will not influence the analysis (Torrence & Compo, 1998).

Finally, all the time series were compared using cross-correlation, cross-spectra, coherence, and phase (Blackman & Tukey, 1958).

Empirical Orthogonal Functions (EOF) were determined for all the time series. The EOF was determined using Singular Value Decomposition method (SVD). This method obtains the variance of each series, maximizing the covariance explained for each mode (Bjornsson & Venegas, 1997). The significance level for retaining EOFs was calculated using Monte Carlo estimate of 95% significance level for a random noise (Jollife, 2002).

Wind

Since wind is one of the most important forces in the area, it is necessary to know the spatial and temporal variability of the wind field. In addition, it is necessary to know if the wind measured at the coastal stations represents the wind field in the study area. To answer these questions wind data obtained by satellite was used for comparison.

Monthly satellite wind data for the area between 15°S to 28°S and 70°W to 85°W during the period of August 1991 to December 2003 was obtained from CERSAT, IFREMER (French Research Institute for Exploitation of the Sea). The data between 1991 and July 1999 was obtained with satellite ERS 1 and has a spatial resolution of 1 degree. The data since August 1999 was obtained with satellite QuikSCAT and has a spatial resolution of 0.5 degree. The data from satellite ERS was interpolated to a regular grid of 0.5 degree using a bi-cubic interpolation. With these data Ekman transport, Ekman depth, wind divergence, and Ekman pumping were calculated.

North-south (v) and east-west (u) components of the wind vector was determined. The component alongshore correspond to the component parallel to the coast, and cross-shore is orthogonal to the coast.

Ekman transport - The total transport results from a balance between the Coriolis force and frictional stress at the surface:

$$\overrightarrow{M} = \frac{\vec{\tau}}{\rho f}$$

where τ is the stress $\vec{\tau} = \rho_a \, C_d \, |\overline{W}| \overline{W}$, ρ_a is the air density, ρ is the water density, C_d is the drag coefficient, $\overline{W}$ is the wind vector, and f is the Coriolis parameter.

Ekman Depth (D_e) was calculated using the equation (Pond & Pickard, 1983):

$$D_e = \frac{3091 \, C_d \, W}{\sqrt{\sin \phi}}$$

where the drag coefficient (C_d) was 1.4×10^{-3}, ϕ is the latitude, and W the wind speed.

In a two layer system—when the surface layer is shallow—we can often assume that the Ekman depth is equal to the depth of the surface mixed layer. This occurs because the strong stratification in the thermocline suppresses mixing and thus the effect of wind stress is confined to the surface layer.

Divergence - The mean divergence of a wind field $\overline{W}$ is:

$$\overline{\nabla} \bullet \overline{W} = \frac{\partial u}{\partial x} + \frac{\partial v}{\partial y}$$

The expansion or spreading out of a vector field; positive values mean convergence (downwelling), and negative values divergence (upwelling).

In meteorology, because of the predominance of horizontal motions, the divergence usually refers to the two-dimensional horizontal divergence of the velocity field. The order of magnitude of the horizontal divergence in meteorological motions is of order $10^{-6}s^{-1}$; the wind field associated with migratory cyclonic systems, $10^{-5}s^{-1}$; motions of smaller scale (such as gravity waves, frontal waves, or cumulus convection) have characteristic divergence one or two orders of magnitude greater.

Ekman Pumping (W_E) was calculated with the curl of the wind stress:

$$W_E = \hat{k} \bullet \nabla \times \frac{\vec{\tau}}{\rho_o f} = \frac{\partial}{\partial x}\frac{\tau_y}{\rho_o f} - \frac{\partial}{\partial y}\frac{\tau_x}{\rho_o f}$$

In the Southern Hemisphere, positive wind stress curl causes convergence in the Ekman layer and downward Ekman pumping; and negative wind stress curl causes divergence in the Ekman layer and upward Ekman pumping.

Even though the Ekman pumping field is influenced by high-frequency weather fluctuations, and contains a large fraction of energy at periods shorter than a few months, it also contains low frequency climate fluctuations.

Climatology

For each parameter of the satellite wind, seasonal and monthly climatologic mean was obtained for the period of ERS (1992-1999) and QuikSCAT (2000-2003). The QuikSCAT seasonal climatology was plotted and discussed.

Physical, biological, and chemical processes

The most important physical, biological, and chemical processes in the area and their relative importance, relevant to pelagic fisheries, were characterized. The data used was from the seasonal oceanographic cruises (Fig. 2, Table 2) made in the area during the period 1993-2002.

The information was reformatted using bi-cubic interpolation in matrices with resolution of 2.2 km in longitude and 11.1 km in latitude, so that they represent the coastal gradient. In

addition, the data were separated into coastal (coast to 30 km) and oceanic (31 to 200 km) areas to create a time series suitable for graphics and statistical analysis. The information used is summarized in Table 1.

The mixed layer depth was determined using the criteria based on constant temperature difference proposed by Monterey and Levitus (1997). The gradient limit to obtain the MLD was 0.5°C/10 m.

Anchovy populations

The density and the vertical and spatial distributions of anchovy schools came from seasonal acoustic evaluations. The source for the environmental data was seasonal cruises. Each variable was reformatted in matrix of longitude and latitude. In addition, the data was separated into coastal (coast to 30 km) and oceanic (30 to 200 km) areas for to create a time series suitable for graphics and statistical analysis.

SATELLITE WIND VALIDATION

The satellite wind data was validated by comparison with the data measured at the coastal station of Arica, Iquique and Antofagasta, and offshore with the TOGA-TAO buoy #32302 located in 18°S and 85.1°W that obtained data between February 1986 and January 1995. To do this comparison, satellite wind data in the grid closest to the position of each coastal station or buoy was extracted. Four time series were prepared and compared by linear regression (1 offshore and 3 nearshore) (Table 3). For the nearshore comparison, the data between 1992 and 2003 was used, but was plotted for the same period as the offshore data. The information was plotted in the Fig. 3 and summarized in Table 3.

Offshore

The offshore comparison (satellite wind with buoy wind) was made for the period 1992 – 1995 using the satellite wind obtained by satellite ERS 1. Since the satellite provides information at 10 m over the sea level and the buoy provide data at 5 m, the buoy data were increased by 7%, following the Smith (1988) method.

The wind speed present a significant correlation at 95% (r=0.85), with a mean difference of 0.44 m s^{-1} and an RMS error of 3.51 ms^{-1} (Table 3 Fig 3a). The wind direction also had a significant correlation at 95% (r=0.43), with a mean difference of 1.3 degree counterclockwise and an RMS error of 0.03 degree (Table 3 Fig. 3b).

These values are smaller compared to the offshore buoy comparisons done with daily data, from QuikSCAT by Ebuchi et al. (2002) (1.0 m s^{-1} in amplitude; and 20 degrees in direction), from NSCAT by Freilich and Dunbar, (1999) (1.3 m s^{-1}; and 17 degrees) and QuikSCAT by Pickett et al., 2004 (1.0 m s^{-1}; and 15 degrees).

Nearshore

The nearshore satellite wind was compared with the monthly mean wind registered in the three coastal stations (Table 3). The comparison was made for the period 1992 to 1998 (ERS) and 2000 to 2003 (QuikSCAT) (Figs. 3c and 3d). For satellite ERS, the wind speed and direction present a negative weak correlation in the three stations, being significant in wind speed at Iquique and Antofagasta (r=-0.3), with a mean difference of 2.3 m s^{-1} and an RMS error of 0.55 m s^{-1} and (Table 3). The wind direction is significant at Arica and Antofagasta with a difference of 58° and 20° respectively.

Table 3

Comparison between satellite wind and *in situ* measured wind. Values correspond to the difference of wind speed and wind direction. r is the linear regression. Values in bold and underline are significant at 95%.

wind difference Offshore		Mean	Std	variance	r	RMS error
Buoy-sat	speed	0.4	0.4	0.2	**0.85**	3.51
	direction	-1.3	5.4	28.7	**0.43**	0.03
Nearshore - ERS (1992 - 1999)						
Arica - sat	speed	1.5	0.9	0.9	-0.12	1.11
	direction	58.1	13.2	174.3	**-0.28**	0.01
Iquique - sat	speed	2.1	1.3	1.6	**-0.23**	0.59
	direction	42.9	12.8	163.8	-0.03	0.01
Antofagasta - sat	speed	2.3	1.3	1.7	**-0.30**	0.55
	direction	19.1	15.3	233.8	**-0.18**	0.00
Nearshore - QuikSCAT (2000 - 2003)						
Arica - sat	speed	0.7	0.5	0.3	**0.48**	3.07
	direction	53.7	8.0	63.5	**0.29**	0.02
Iquique - sat	speed	1.6	0.9	0.7	0.22	1.35
	direction	41.8	6.5	42.2	**0.57**	0.02
Antofagasta - sat	speed	1.7	1.2	1.3	-0.20	0.73
	direction	13.1	4.3	18.6	**0.35**	0.05

In the QuikSCAT period, the nearshore wind speed and direction present a better correlation than ERS. The wind speed is significant at 95% only at Arica (r=+0.48), with a mean difference of 0.7 m s^{-1} (Table 3). The wind direction presents significant correlation in all the stations with a mean difference of 40 degrees. The differences determined here are comparable with those obtained by Pickett et al. (2004) in the nearshore, using daily data, they found in average 3.1 m s^{-1} in amplitude, and 41 degrees in direction.

In the nearshore case, satellite ERS does not represent the coastal information well. In the coastal stations the maximum is in spring and summer and in the nearshore is in winter, being stronger near or on the coast. This notable difference decrease from Arica to the south, being in phase and with the wind stronger in the nearshore than at the coast at 30°S (Shaffer et al., 1999; Hormazabal et al., 2001). There is probably a similar pattern from Arica to the north area.

On the other hand, QuikSCAT data represent the nearshore wind speed in phase with the coastal stations, even though the correlation is weak. Moving away from the coast the pattern changes and the correlation is negative.

With the available data it was not possible to find the function that represents the bias between ERS and QuikSCAT. For this reason, the time series that include all the period (1992-2003) should be used carefully. To determine the anomaly in a latitudinal transect the climatology of ERS and QuikSCAT periods was used separately.

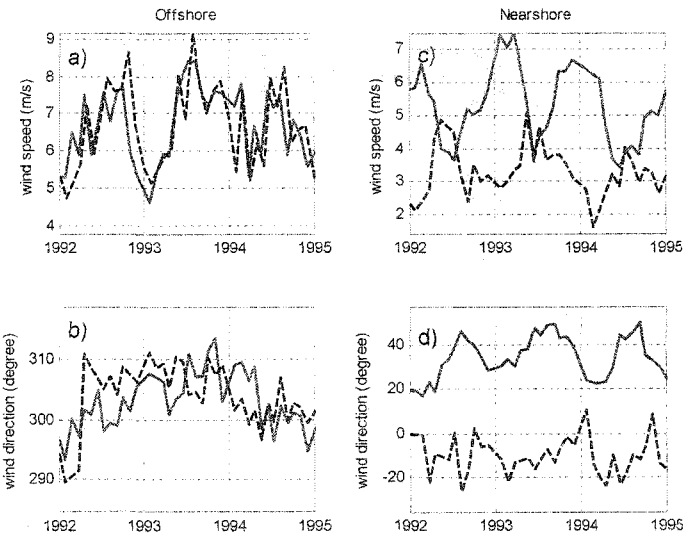

Fig. 3. Comparison of satellite wind (dash line) comparison with offshore (a) wind speed and (b) wind direction buoy wind (solid line) and with nearshore (c) wind speed and (d) wind direction Iquique coastal station wind (solid line).

RESULTS

COASTAL STATIONS - ANNUAL CYCLE

The annual cycle obtained from the monthly climatological means of SST and wind velocity at the three coastal stations (Arica, Iquique, and Antofagasta) and sea level at the coastal stations of Callao and Antofagasta are presented in Fig. 4. The alongshore wind velocities at three locations (Fig. 4d) are maximum (4.2-6.2 m s^{-1}) in late austral spring to summer (December - March) and minimum (2.6-4.0 m s^{-1}) in austral winter (June-July). The cross-shore winds have a similar cycle, but are weaker and have a smaller seasonal range (Fig. 4c). The alongshore component is equatorward and therefore upwelling favorable throughout the year in these climatological monthly means. Daily data (not shown) indicate that poleward winds (downwelling favorable) do occur in winter with timescales of several days and with a latitudinal dependence, occurring more often at Antofagasta than at Iquique and almost never at Arica. The wind is weaker in Arica, which is produced by the change of direction of the coastline that presents a curvature with an approximated radius of 600 km.

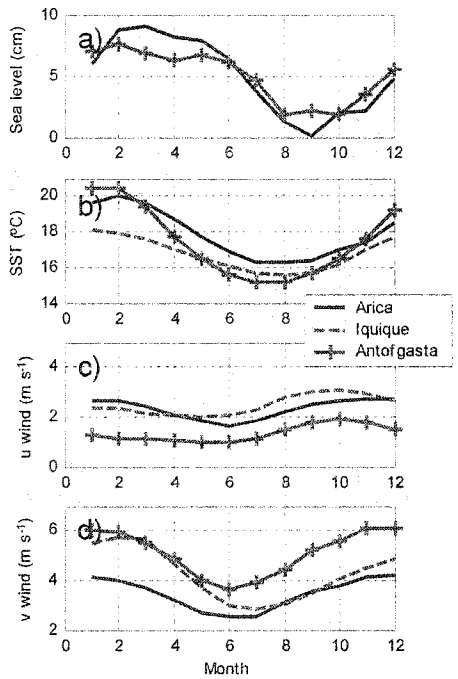

Fig. 4. Monthly average data from coastal stations at Arica (solid line), Iquique (dotted line) and Antofagasta (crosses and solid line) of (a) sea level (Callao and Antofagasta only), (b) sea surface temperature, (c) cross-shore wind velocity, and (d) alongshore wind velocity.

The SST (Fig. 4b) at the coastal stations is in phase with the annual solar heating cycle (maximum in summer). It is similar to the annual wind cycle but with a wind delayed by one month throughout the region. The minimum SST (15.2° - 16.0°C) is in July-September and maximum SST (18.0° - 20.5°C) in January-February. The delay between the wind and the temperature can be caused by the beginning of the upwelling, which maintains SST low whereas winds increase in spring, before the seasonal heating dominates the upwelling.

The annual cycle of the sea level at Callao and Antofagasta (Fig. 4a), shows a seasonal maxima caused by heating and expansion of the water column in summer. Minimum sea levels lag those of temperature by 1- 2 months, with lowest values in late austral winter and early spring (August-October). This lag may be the result of the alongshore northward current that intensifies in spring, generating a cross-shore geostrophic slope that keeps the sea level low. The maximum values of the summer happen in February and continue high until August.

Thus, the seasonal cycle here is a balance of the upwelling wind cycle and the heating and cooling cycle.

COASTAL STATIONS - VARIABILITY

Fig. 5 shows the raw data of selected variables and places that are sufficiently long to illustrate the variability. In each series, the principal part of the variability corresponds to the seasonal cycle, especially in the series of temperature, wind, and atmospheric pressure. In these series, the seasonal variability represents between 50 and 80% of the total variance. On the other hand, the quadratic trend only explains between the 0.5 and 2% of the total variance. In the sea level time series, the seasonal cycle is very small and the variance of the quadratic trend can reach 8% of the total variance.

The standardized residual obtained by STL (Fig. 6) represents between 10 and 40% of the total variance. This residual is similar to the anomaly determined through the subtraction of the quadratic trend and the monthly mean. The difference between both methods is around 2 to 5%, and the STL residual present smaller variance. The STL residual shows a sequence of positive and negative changes, generated principally by ENSO and other unidentified processes. There are significant anomalies in all the series of more than two standard deviations. They are caused by the El Niño of 1982-83 and 1997-98. The warm events of 1972-73, 1976-77, 1986-87, 1991-92, 1994, and 2001-02 show anomalies do not exceed two standard deviations. The cold event 1964, 1971, 1974-75, 1984, 1989, 1996, 1999, and 2002 also present anomalies less than 2 standard deviations. Another remarkable situation in these series is the conclusion of the 1972-73 event. At that time a significantly lower sea level (less of -2 standard deviations) was seen at Callao and

Antofagasta (Figs. 6f and 6g). The anomaly was associated with an increment of the atmospheric pressure in Antofagasta (Fig. 6i) and with a positive SOI. This event could be caused by an extraordinary intensification of the northward coastal flow. This change observed in sea level coincided with small anomalies in the coastal station wind and SST.

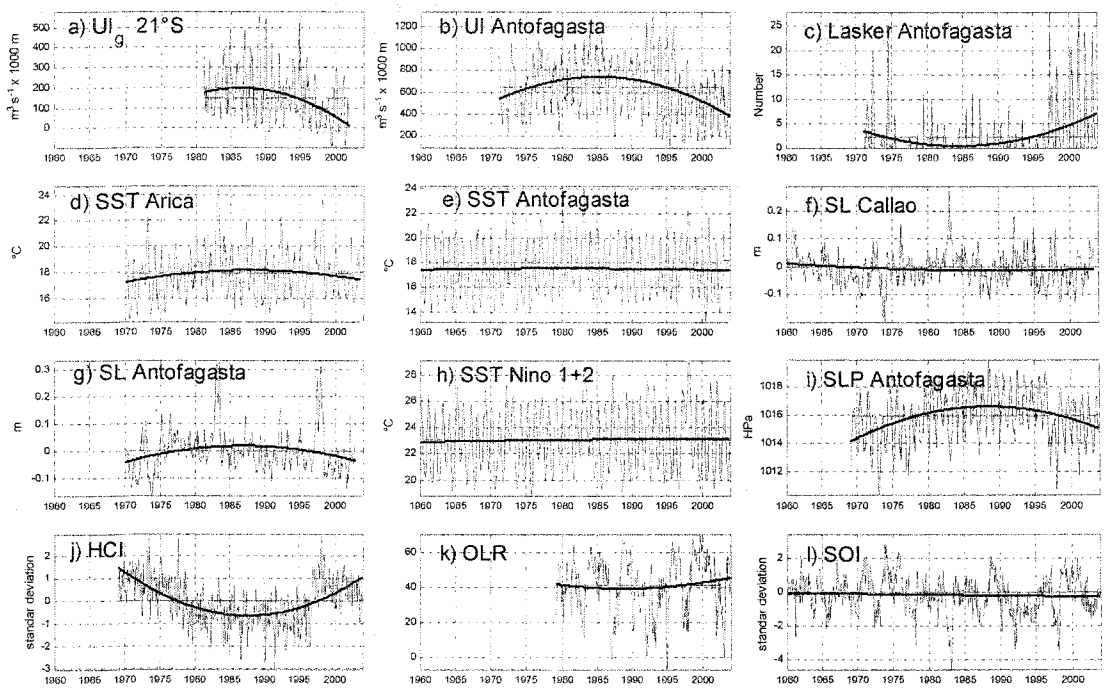

Fig. 5. Average of raw data (segmented line), quadratic trend (thick line) and monthly mean data (thin line): (a) Upwelling Index of geostrophic wind (Pacific Fisheries Environmental Laboratory product) 21°S and 71°S, (b)Upwelling Index at Antofagasta coastal station, (c) Lasker events at Antofagasta coastal station, (d) SST at Arica coastal station, (e) SST at Antofagasta coastal station, (f) Sea level at Callao coastal station, (g) Sea level at Antofagasta coastal station, (h) SST Nino 1+2 area, (i) Atmospheric pressure of Antofagasta coastal station, (j) Humboldt Current index (HCI), (k) Outgoing longwave radiation (OLR) and (l) Southern oscillation index (SOI).

The seasonality in the time series accounted for 50 and 80% of the total variance. Normally the seasonality is eliminated from the time series when the anomaly is determined, assuming that it is constant in time. By that reason, STL method has an enormous potential as data analysis tool, because it separates each component of the series. Fig. 6 shows the seasonality

of some of the series. It is possible to see that the amplitude of the seasonal cycle changes with time. In some cases it reduces the amplitude (Fig. 7a) or increases the amplitude (Fig. 7b) of the annual cycle. That change in the amplitude is produced because the seasonal trend of the monthly mean values for winters is different from the seasonal trend for summers. This is similar to case of the sea level atmospheric pressure at Easter Island (not shown) that was used to calculate the HCI (Fig. 7j).

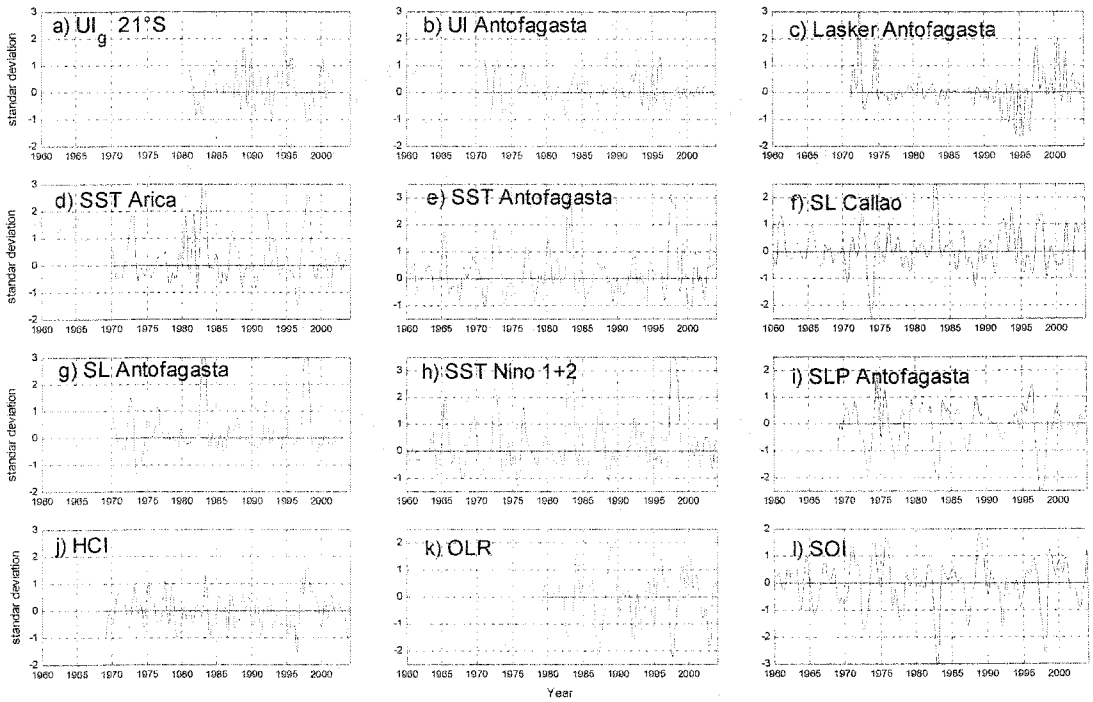

Fig. 6. Standardized STL residual of monthly mean data from: (same as Fig. 5). Data smoothed with a 5 months fourth order bidirectional Butterworth low-pass filter.

Fig. 8 is an example of the quadratic trend changes for each month in the SST at Antofagasta. During spring and summer months, the temperature trend decreases and in the winter the trend increases.

The standardized long-term trend obtained by STL is plotted in Fig. 9 and synthesized in Table 4. This long term anomaly in most of the cases reaches two standard deviations, with cycles of the order of 40 to 50 years (20-25 years half cycle) that correspond to the interdecadal variability and represents the changes of regime (regime shift). All the series show 3 regimes: one cold, before 1976, another warm between 1976 and 1998 and the last one, a cold period

beginning in 1998 (Table 4). Coincident regimes are found in the North Pacific Ocean (Bond et al., 2003; Chavez et al., 2003; Peterson and Schwing, 2003). Additionally, these changes are coherent with the anchovy and sardine cycle (Fig. 1). In the variables that represent the ocean (Figs. 9d to 9h), a change or alteration is also observed during 1989, but this change is not observed in the meteorological variables (Figs. 9a to 9c, 9i, 9j). The long-term trend in the last years shows a diminution of the upwelling index, SST, SL, and SLP, and an increment of the Lasker events (calm).

Table 4

Interdecadal trend in the time series from northern Chile and some indices. The year limit of each period is approximated. Symbol + or - indicates the sign of the anomaly during this period

	< 1976	1976 - 1998	> 1998
Coastal wind	-	+	-
Coastal Lasker		-	+
Geostropic wind 18°S		+ | -	+
Geostropic wind 21°S		+	-
SST coastal	-	+	-
SL coastal	-	+	-
SST Nino 1+2	-	+	-
SST Nino 3.4	-	+	-
SOI	+	-	+
PDO	-	+	-
QBO	-	+	-
AP Eastern	+	-	+
AP Antofagasta	-	+	-
HCI	+	-	+
Anchovy	+	- | +	+
Sardine	-	+ | -	-

The MEM spectral analysis of the time series without trend (Fig. 10) shows peaks at several frequencies representing 3 identifiable bands of variability: biennial or quasi-biennial (1.5-3 years), ENSO (3 to 8 years), and decadal (9-12 years). Eliminating the trend of the series (by STL method as by the quadratic method) eliminates the maximum of high energy in the interdecadal scale (12 to 25 years or greater). This methodology determines with a better degree of significance the variability with periods shorter than 12 years.

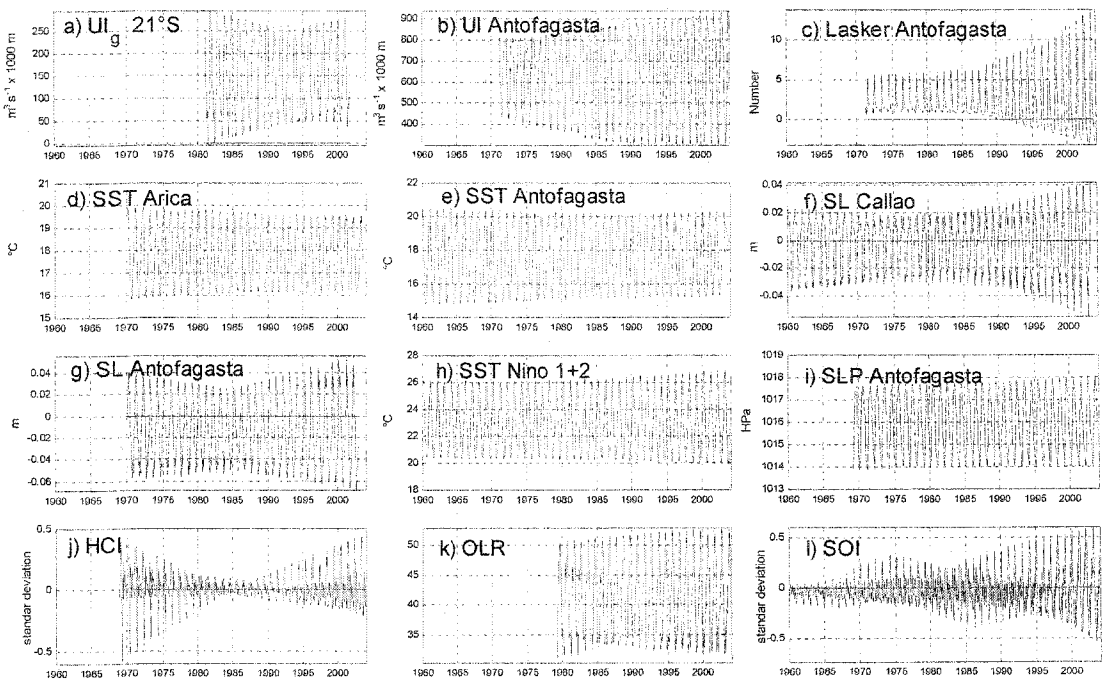

Fig. 7. Seasonality of monthly mean data (same as Fig. 5).

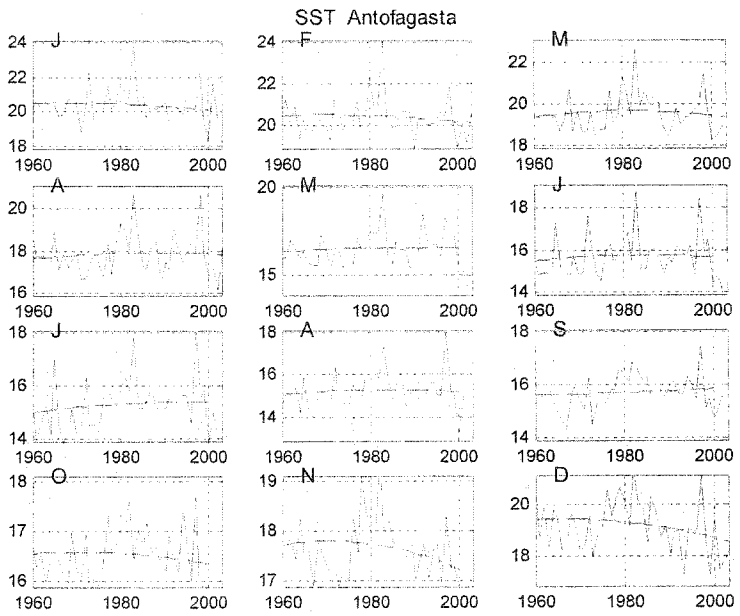

Fig. 8. Monthly mean variability and quadratic trend of SST at Antofagasta.

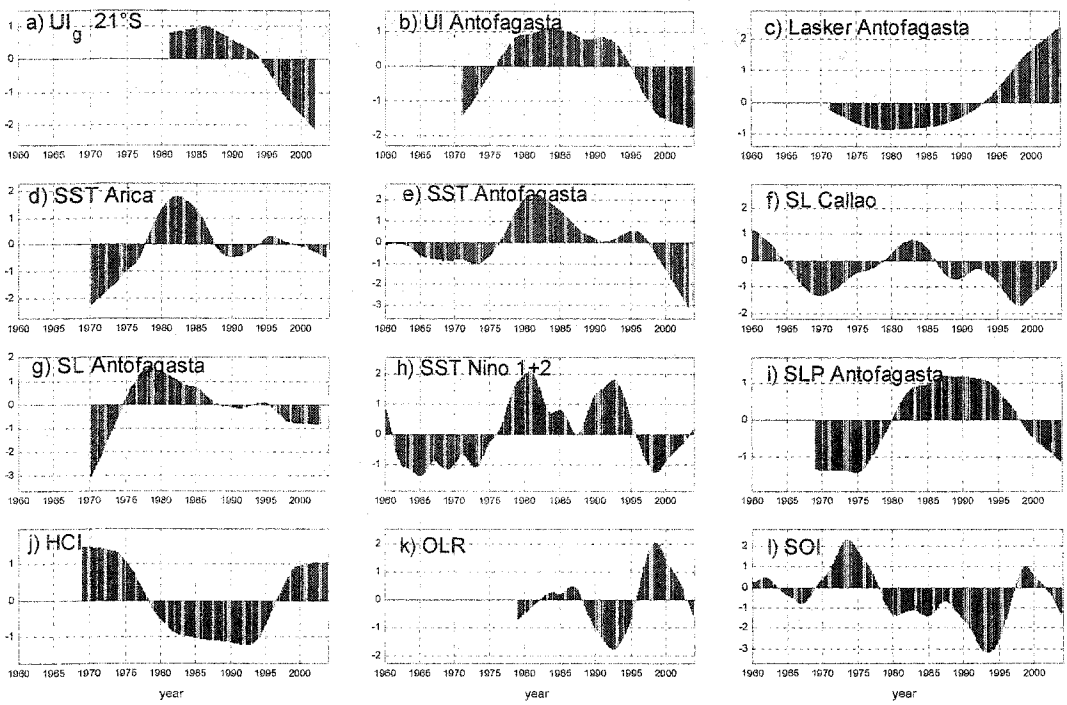

Fig. 9. Standardized STL trend (10-year filter) of monthly mean data (same as Fig. 5).

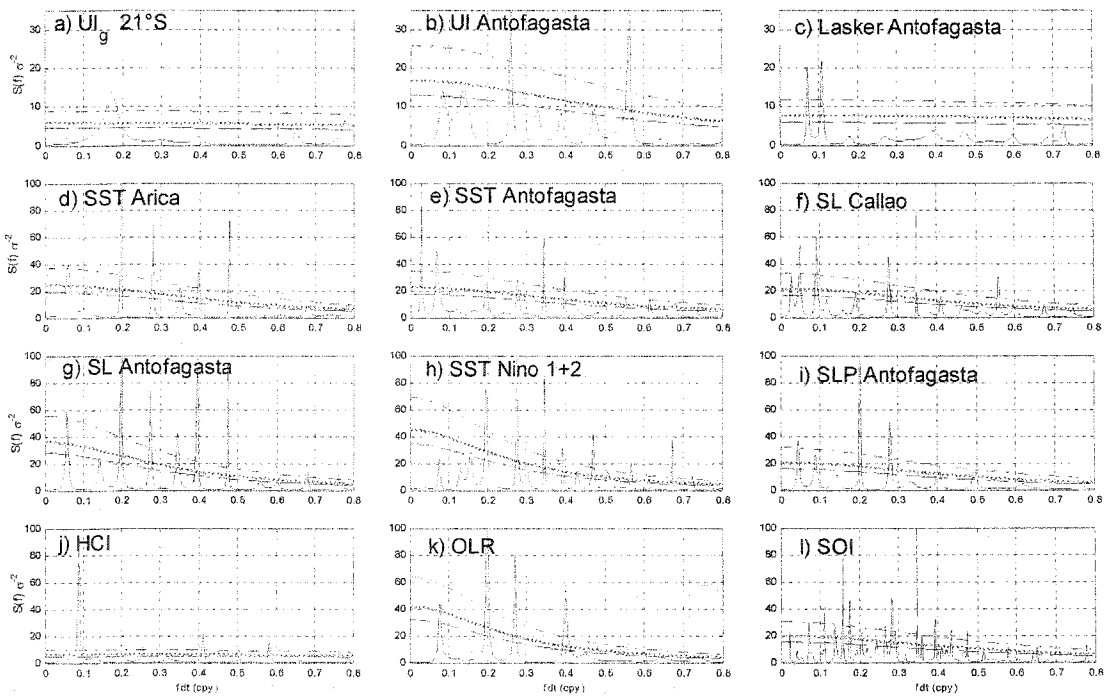

Fig. 10. Maximum entropy spectrum of monthly mean anomaly (same as Fig. 5). Horizontal segmented, dot and segmented-dot lines represent 90%, 95%, 99% confidence levels.

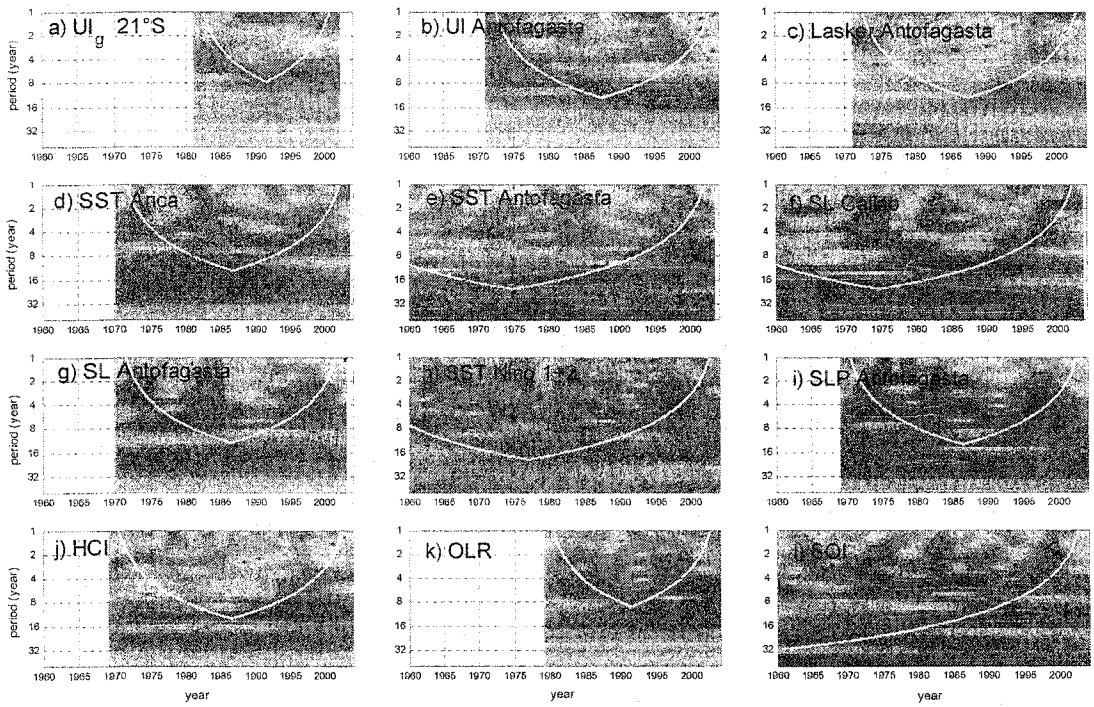

Fig. 11. Wavelet analysis (white thick line > 95% confidence) of monthly mean data (same as Fig. 5). Dark colors are maximum energy.

The wavelet analysis (Fig. 11) shows the maximum energy at the same frequency bands as that obtained with MEM, and additionally indicates the times those frequencies were observed. Note that the variations of the quasi-biennial frequency occur mainly during the El Niño events and that the variations at frequency bands of ENSO, decadal and interdecadal are present during almost all the time. Using the wavelet methods the signal was separated by frequency and was integrated over the band of 2 to 8 years (biennial and ENSO) (Fig. 12) and over the band of 10 to 17 years (decadal) (Fig. 13). Additionally, in each band the variation, winter and summer variability was determined separately. In the frequency band of ENSO (Fig. 12) the total signal (thin line) has a maximum variance during the El Niño events of 1972-73, 1982-83 and 1997-98. The variance of summer and winter does not follow the total signal, and they do not exhibit differences among them either, with exception of the series HCI (Fig. 12*j*), where winter in the 80's present more energy than summers. On the contrary, in the middle of 1990's the summers have a larger variance. In the band of the decadal variations (Fig. 13), the difference of variance between the total signal and winter and summer is similar in some cases (Figs. 13*d*, 13*c*),

however, in most of the series, this variance is different (Figs. 13*a*, 13*b*, 13*c*, 13*h* to 13*l*). These results confirm that the changes in the seasonality are governed by decadal variations.

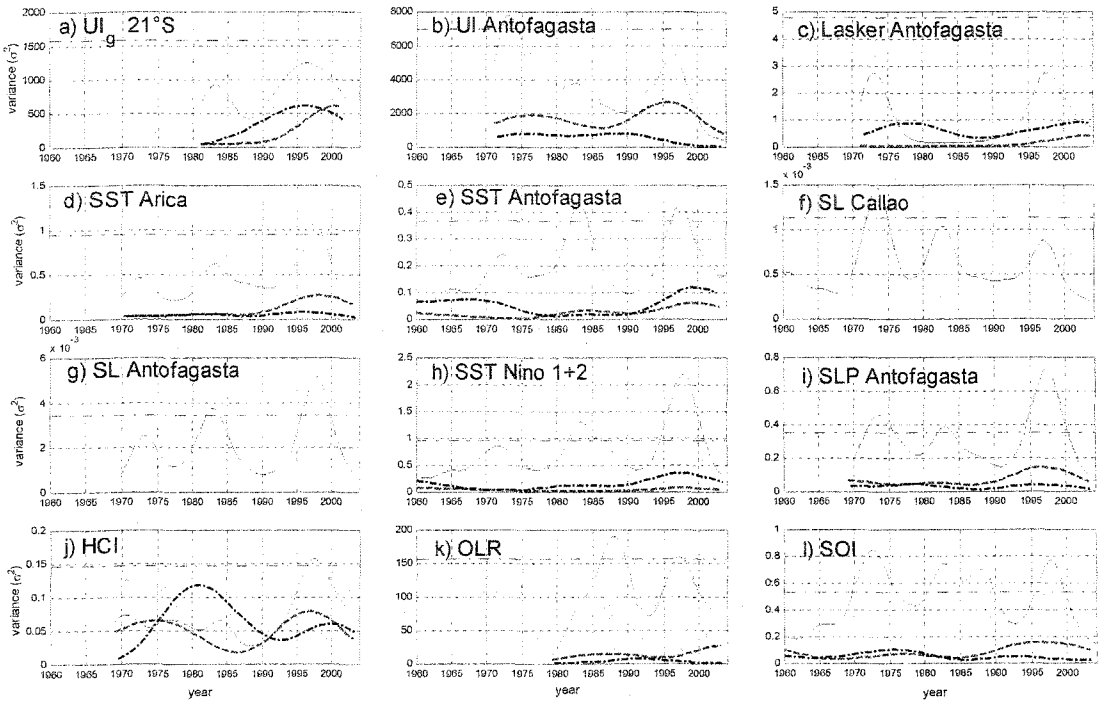

Fig. 12. Wavelet variance for the 2 to 8 year period (continuous line), summer (January - March) (segmented line), and winter (July – September) (segment dot line) of monthly mean data (same as Fig. 5).

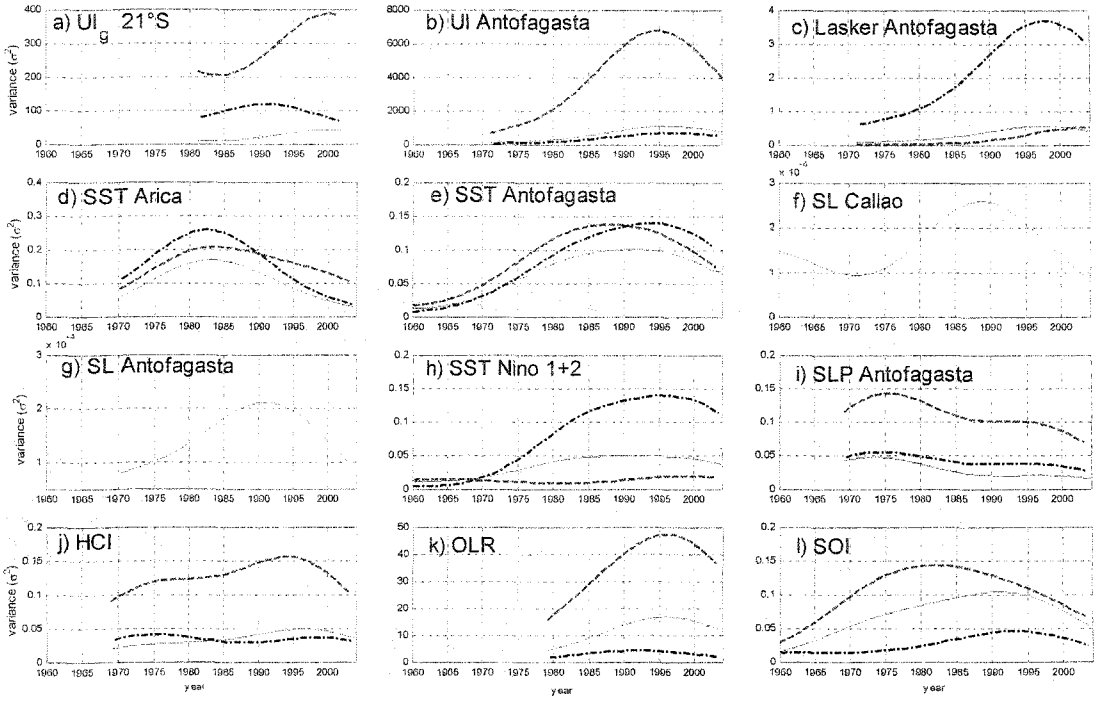

Fig. 13. Wavelet variance for the 10 to 17 year period (continuous line), summer (January - March) (segmented line), and winter (July – September) (segment dot line) of monthly mean data (same as Fig. 5).

In general, there is a good correlation between all the analyzed series. Fig. 14 shows the correlation, cross spectra, coherence, and phase between -SOI and SST, sea level and upwelling index at Antofagasta and Fig. 15 between the OLR and the same variables. In both cases the correlation is negative and shows peaks in the cross spectrum with a high coherence in the bands of the quasi-biennial, ENSO and decadal with differences of phase between 0.5 and 3 years. Other correlations (not shown) indicate a positive correlation between the sea level and the SST at Antofagasta, with a phase lag of one month. Nevertheless, in the long term, the correlation with high coherence is negative in the 2.1 and 4.5 years bands and positive in the 2.8 and 7.6 years bands. These correlations confirm the complexity of the system and illustrate that the study region is affected by both local and remote forcing.

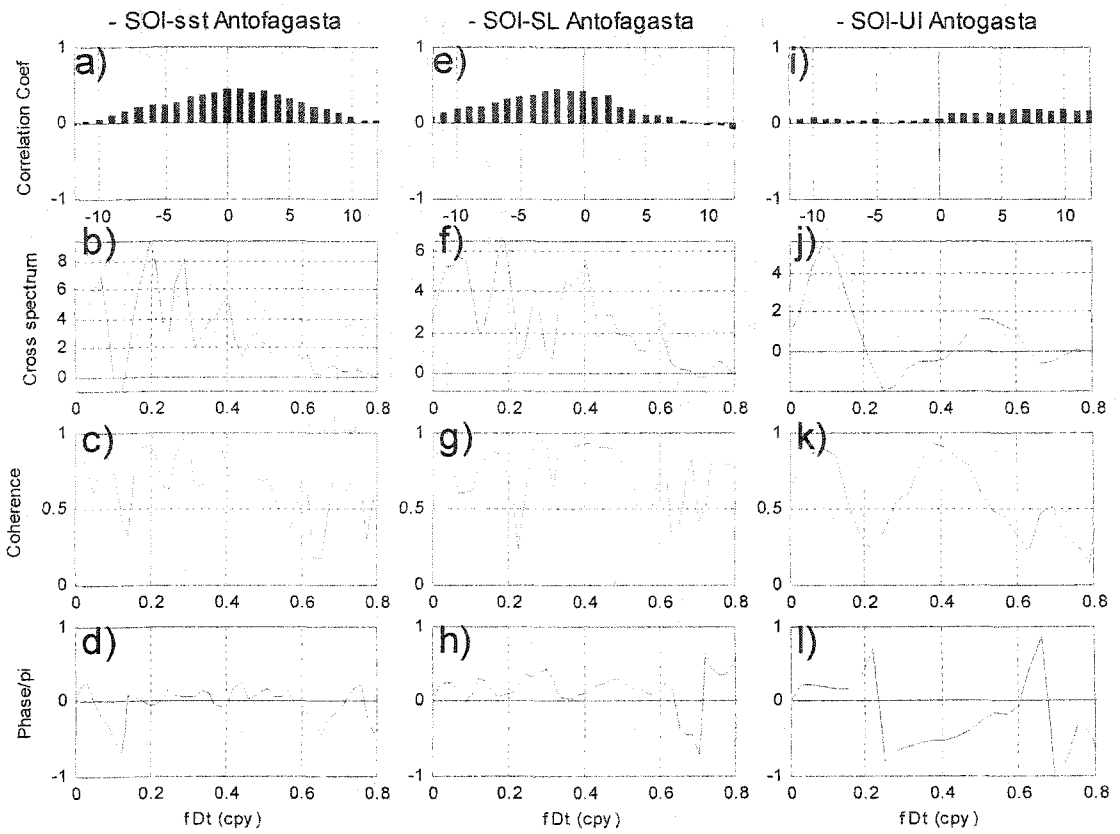

Fig. 14. Lagged correlation of monthly data (a,e,i), cross spectrum of anomalies (b,f,j), coherence (c, g, k) and phase (d, h, l) between monthly time series of –SOI (negative) and SST, SL and UI at the Antofagasta coastal station.

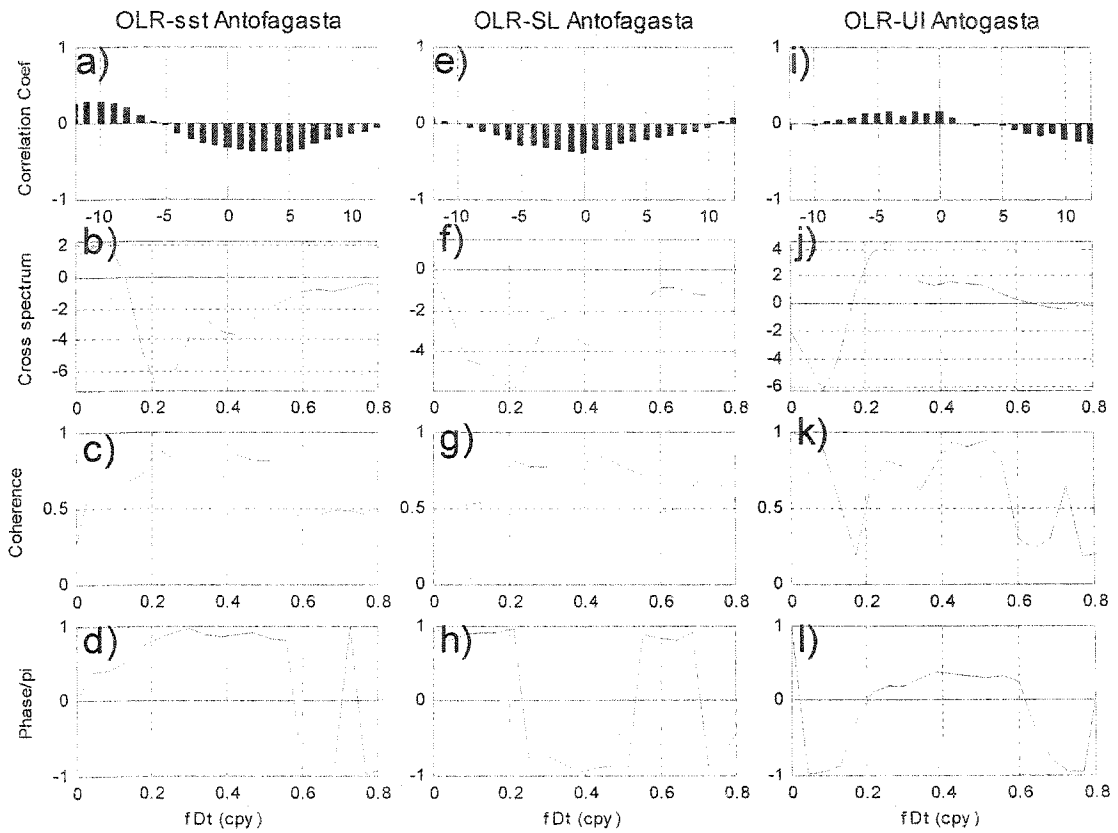

Fig. 15. Lagged correlation of monthly data (a,e,i), cross spectrum of anomalies (b,f,j), coherence (c, g, k) and phase (d, h, l) between monthly time series of OLR and SST, SL and UI at the Antofagasta coastal station.

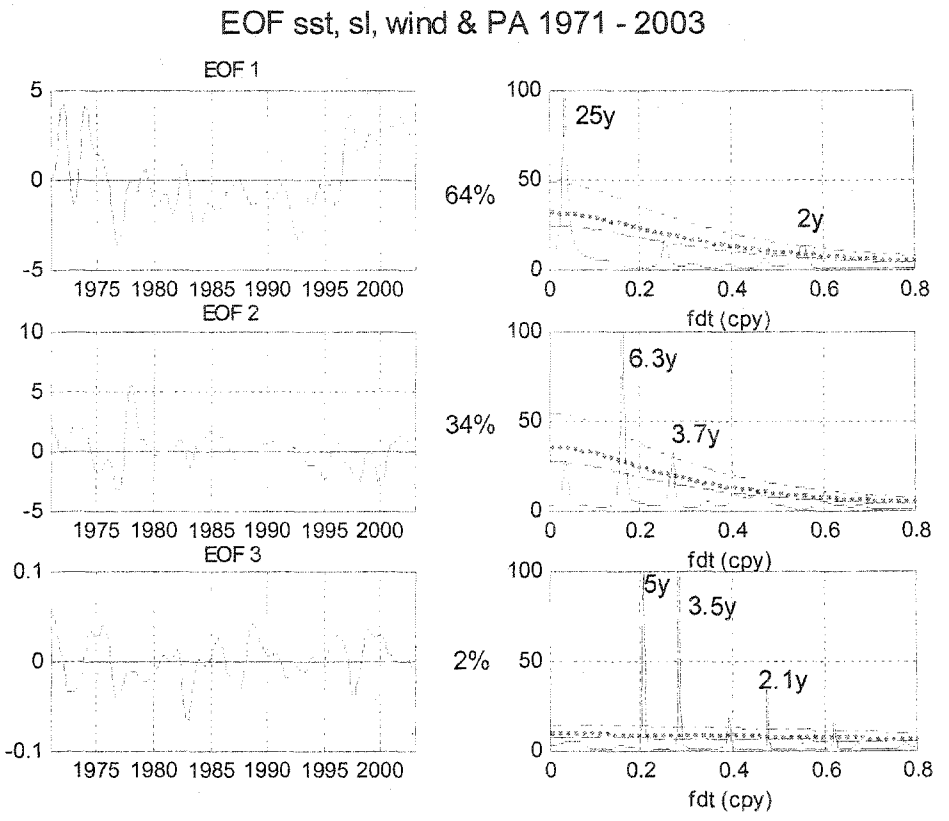

Fig. 16. First three EOF modes and their spectrum for the monthly time series of SST, SL, winds and SLP for the period 1971 to 2003 in northern Chile.

The EOF analysis of all the coastal stations time series (SST, SL, wind and SLP) for the period 1971 to 2003 (Figs. 16) shows that the first mode explains 64% of the variance and corresponds to the interdecadal variations (20 to 30 years) with an important influence of the variations in quasi-biennial scale. The second mode explains 34% of the variance and represents the variations in ENSO scale. Even mode three shows changes in the ENSO band, but this mode is not significant and it would not contribute to the total variance. The first two EOF modes explain 98% of the variance.

The relation between the environment variables and the annual landing of anchovy and sardine in northern Chile were obtained by (a) correlation and (b) lagged correlation (Table 5). In some cases, the sign of the correlation when the two variables are in phase is different than when the maxima correlation occurs (e.g. SST & anchovy; SL & Anchovy). Also in the case of the UI, different behavior between Arica, Iquique, and Antofagasta is observed (Table 5).

Table 5

Correlation between environmental time series and anchovy and sardine landings. (a) On phase, (b) maximum correlation coefficient (lag in years).

	Anchovy		Sardine	
	(a)	(b)	(a)	(b)
SST	-	+4	+	+2
SL	-	+8	+	+2
UI (1)	+	-2	-	+5
UI (2)	-	+7	+	-5
Lasker	+	-3	-	+4
SOI	+	+3	-	+2
SLP	+	+4	-	-2
HCI	-	-1	+	+10
OLR	-	-3	+	-2

UI (1) : Upwelling index in Arica
UI (2) : Upwelling index in Iquique and Antofagasta

SATELLITE WIND - SEASONAL SPATIAL CLIMATOLOGY

Satellite winds provide a valuable spatial view of the wind field not provided by the coastal and buoy stations. The alongshore wind field has two maximums of intensity, separated by a minimum (Fig. 17). The first maximum is centered at 15°S and the second at 28°S, where the values reach more than 10 ms^{-1} in winter. In these areas, the wind speed at the shore stations is less than at nearshore. The minimum, in the area between 17 and 24°S, has intensities less than 5 ms^{-1}. In this particular area, the wind intensity at the coast is higher than at nearshore area (Figs. 4d and 17), because along the coastline the wind is accelerated thermally. The seasonal climatology show that the maximum values appear in winter-spring and the minimum in summer, increasing from the coast towards the ocean. The wind direction is predominantly toward the north and northwest, following the coastline (Fig. 17). The Ekman transport in all the area is negative (Fig. 18) (offshore). The maximum offshore transport takes place north of 18°S, reaching values less than -2 $m^3 s^{-1}$ in winter. The minimum values are observed nearshore between 18 and 26°S in summer.

The wind divergence in the area is mainly positive (convergence = downwelling) and with a maximum in winter in the oceanic area south of 24°S (Fig. 19). The intensity decreases in the spring. The maximum also appears in the oceanic area, but towards the North zone. The

negative divergence (divergence - upwelling) is observed throughout the coast, specially in summer, in the area north of 23°S and south of 27°S. The divergence diminishes remarkably in fall, where divergence is only observed is some coastal areas, being reduced even more in winter and spring. The coastal areas between 20 - 22°S and 26 - 28°S have divergence all the year.

The Ekman pumping (Fig. 20) has the maximum (positive = downwelling) in the winter in the oceanic southern area, decreasing in summer. Negative values (upwelling) are observed all the year in a band of about 600 km wide along the coast. Negative values in the Ekman pumping are associated with a positive wind stress curl or coastal divergence.

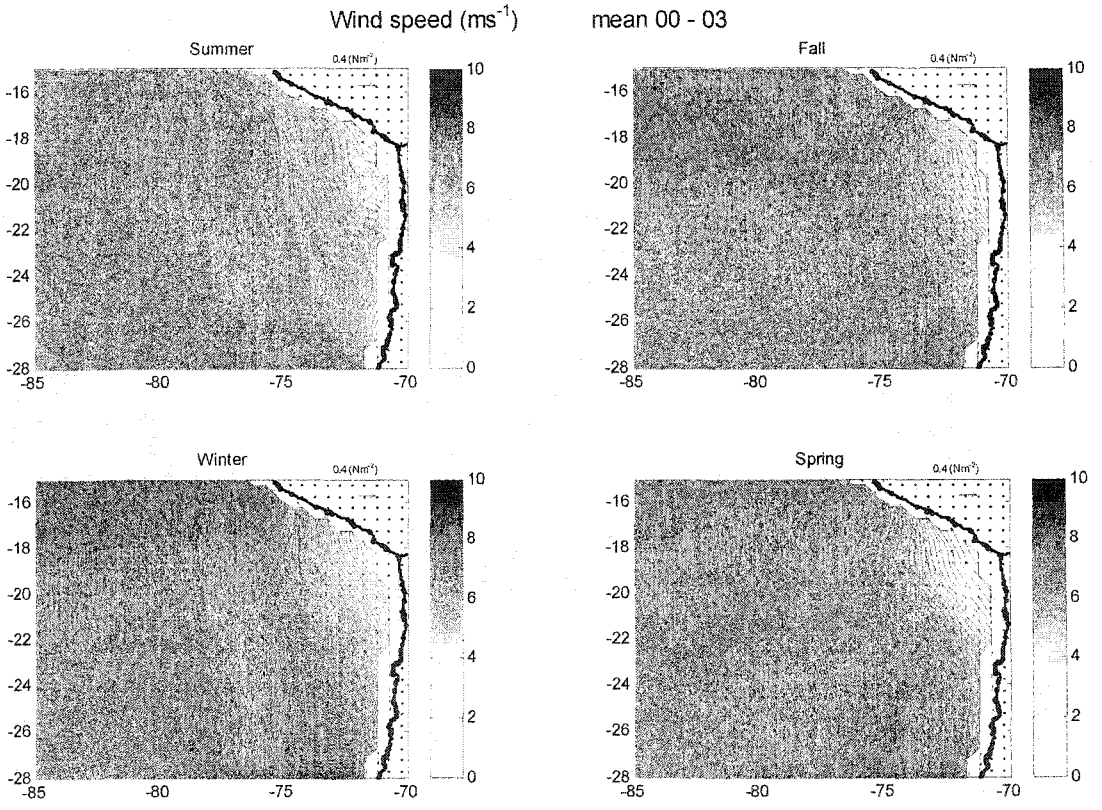

Fig. 17. Satellite wind speed seasonal climatology (contour and color). Mean from the period 2000 to 2003. Resolution half degree. Arrow represents the wind stress vector.

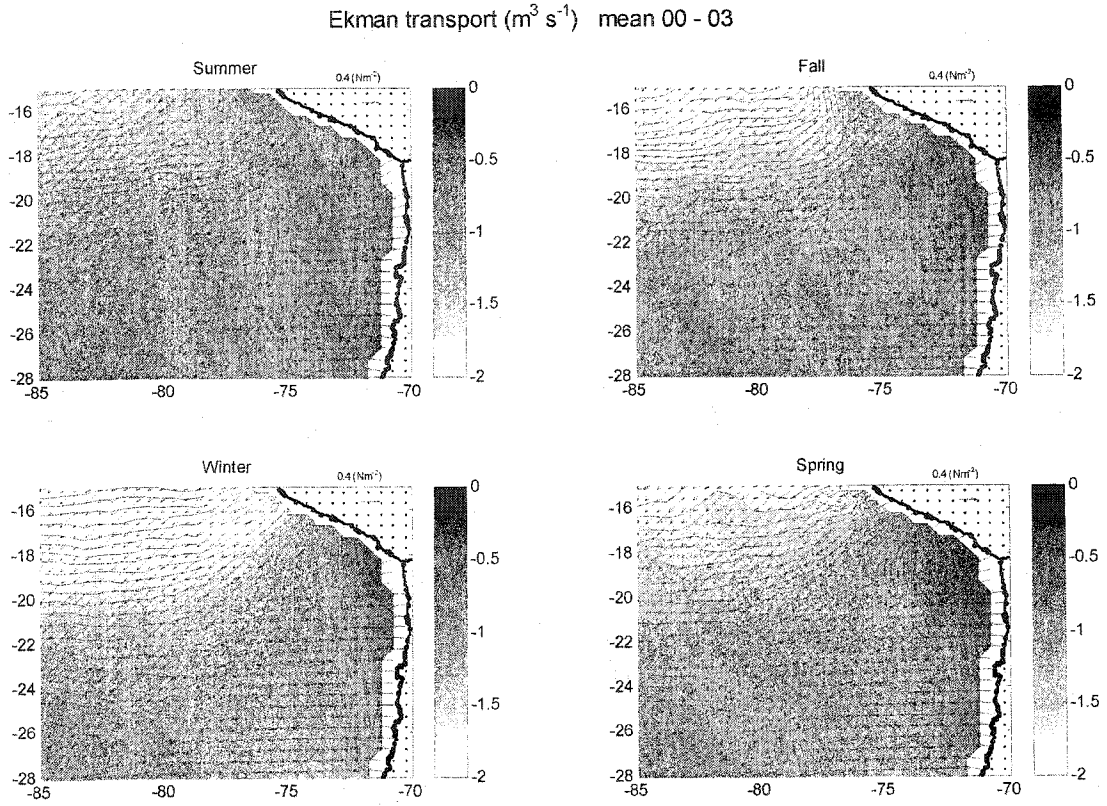

Fig. 18. Satellite wind Ekman Transport seasonal climatology (contour and color). Mean from the period 2000 to 2003. Resolution half degree. Arrow represents the Ekman transport vector.

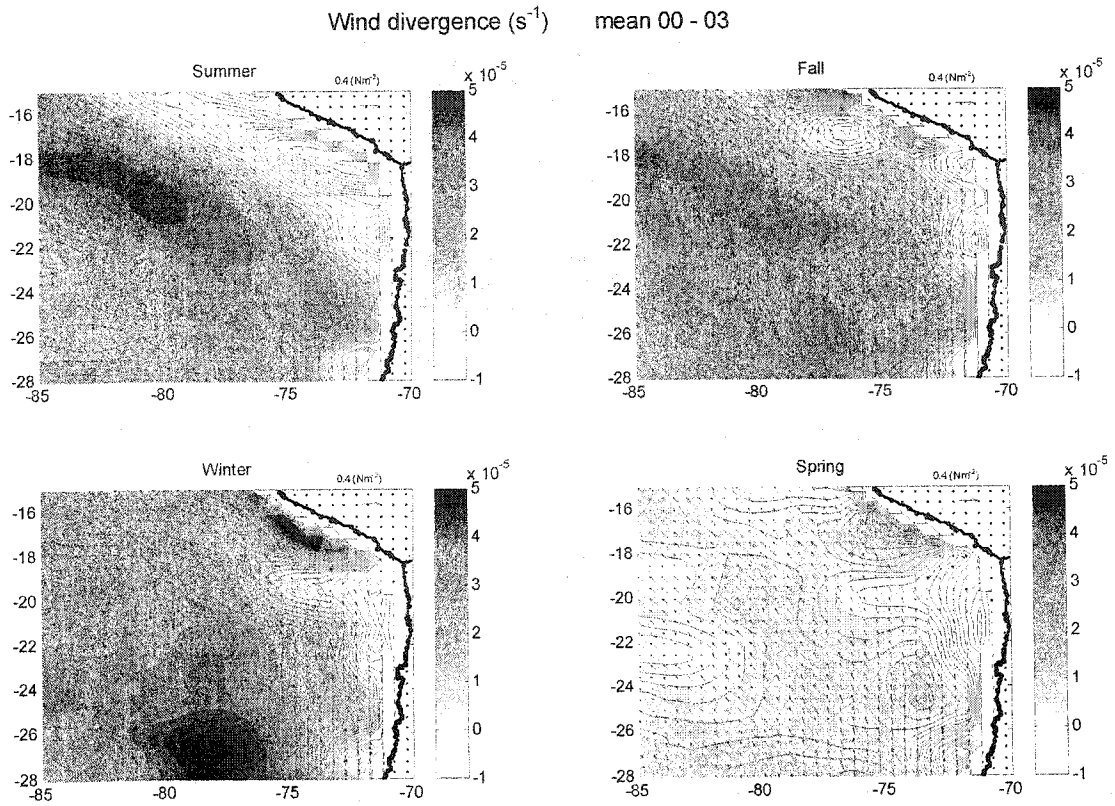

Fig. 19. Satellite wind divergence seasonal climatology (contour and color). Mean from the period 2000 to 2003. Resolution half degree. Arrow represents the wind stress vector.

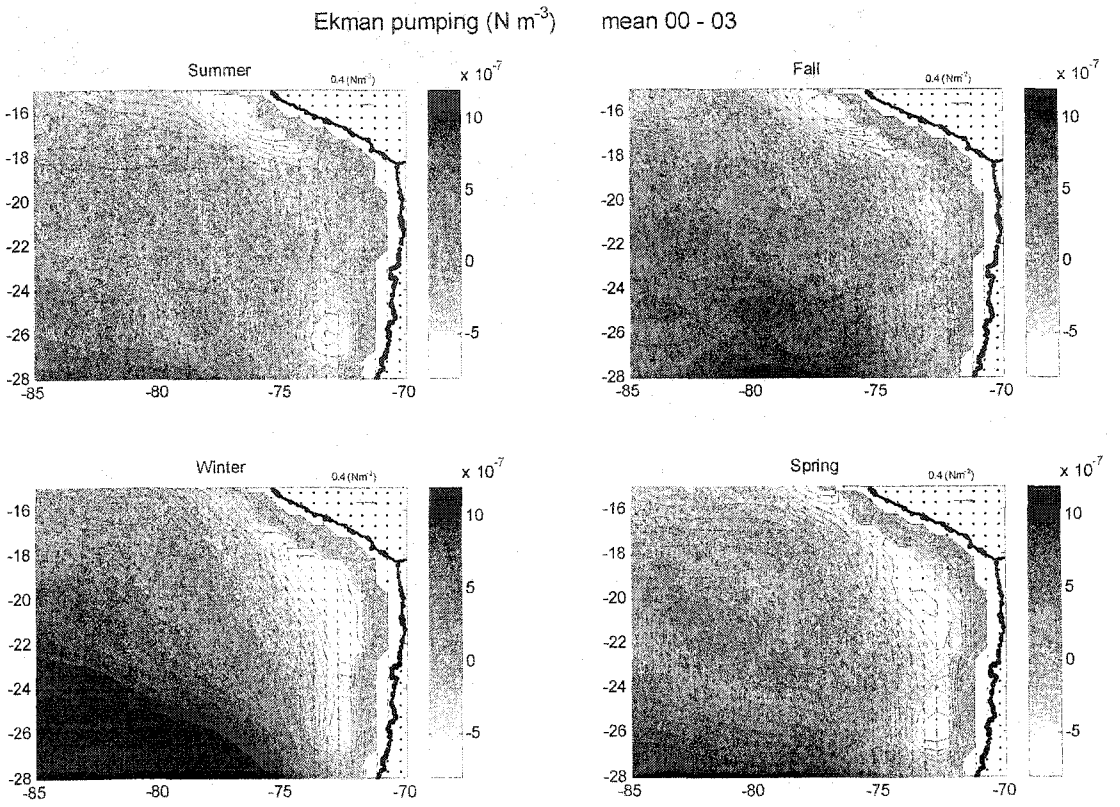

Fig. 20. Satellite wind Ekman pumping seasonal climatology (contour and color). Mean from the period 2000 to 2003. Resolution half degree. Arrow represents the wind stress vector.

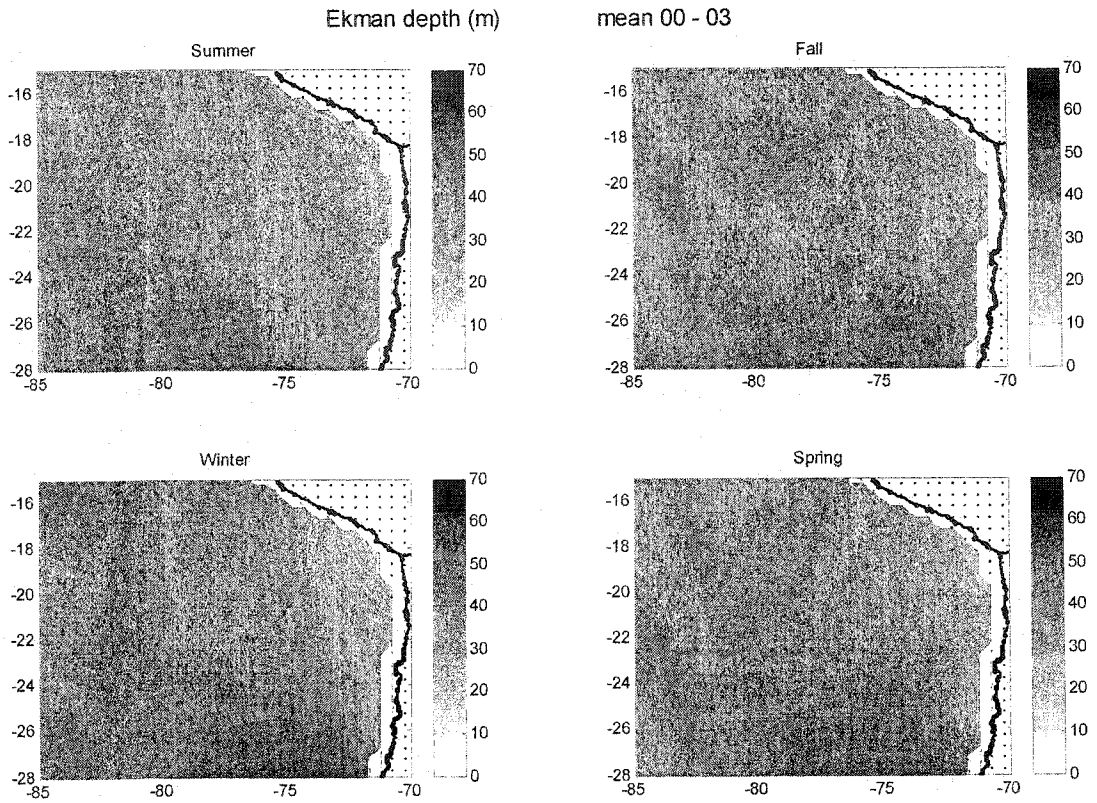

Fig. 21. Ekman layer depth seasonal climatology (contour and color) estimated with satellite wind. Mean from the period 2000 to 2003. Resolution half degree. Arrow represents the wind stress vector.

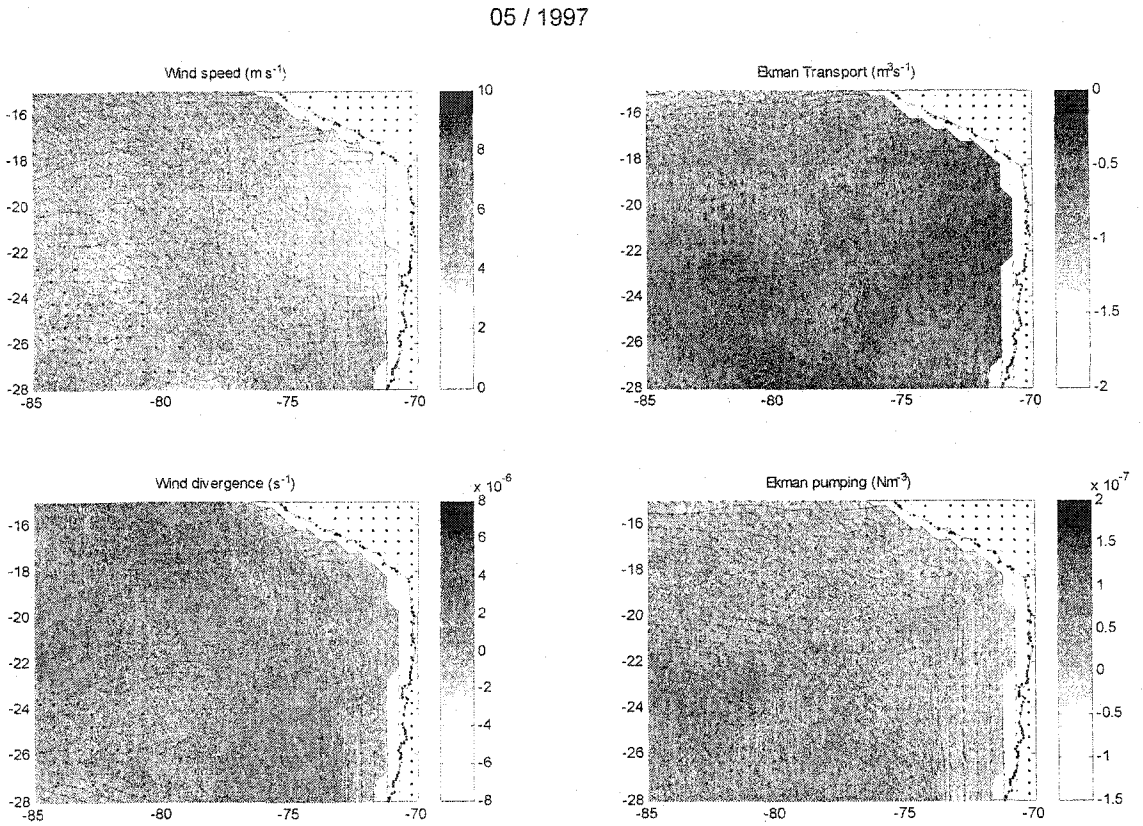

Fig. 22. Wind speed, Ekman transport, divergence and Ekman pumping of the wind obtained by satellite during the beginning of El Niño conditions (May 1997).

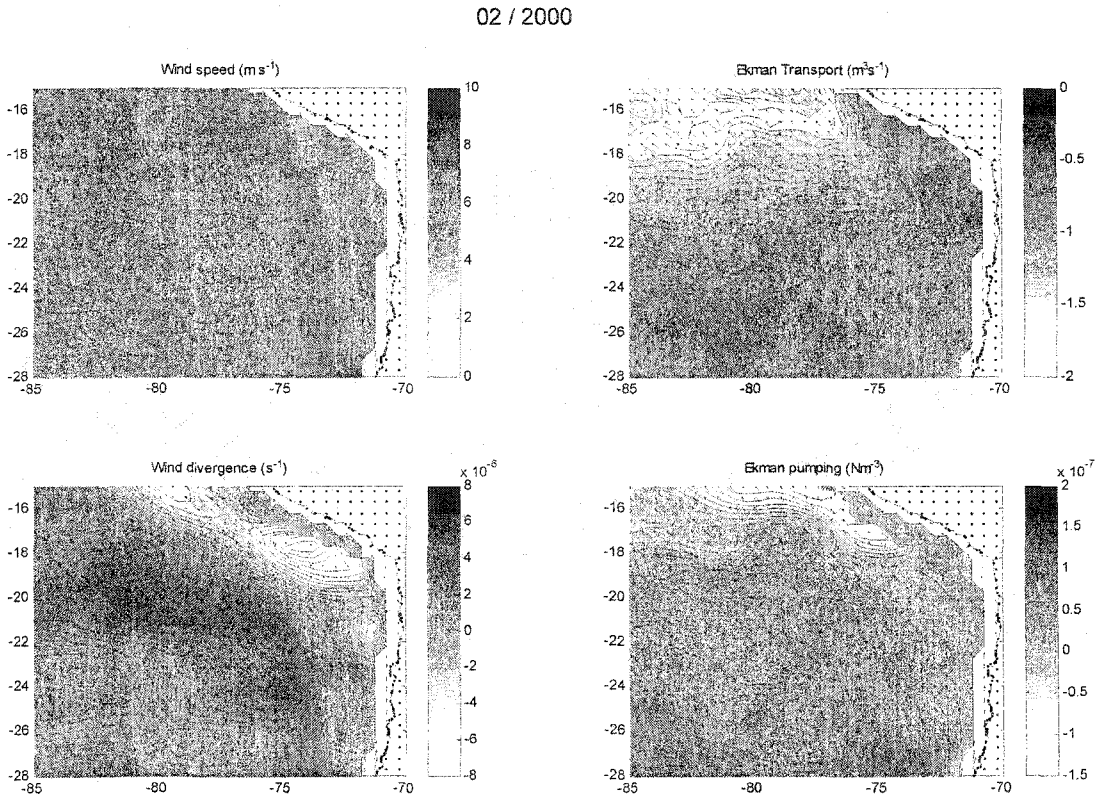

Fig. 23. Wind speed, Ekman transport, divergence and Ekman pumping of the wind obtained by satellite during La Niña conditions (February 2000).

The Ekman layer depth (Fig. 21), show that the depth increases from the coast (< 30 m) to offshore (> 40 m). The maximum depth (> 60 ms) is observed in winter south of 28°S.

The general pattern just described by the climatology is altered during ENSO events. For example, during the beginning of the El Niño (May 1997) there was a remarkable diminution in the wind intensity and in the offshore transport, divergence and Ekman pumping (Fig. 22). The opposite case, wind intensification, can be observed during La Niña events (e.g. February 2000). In the case shown in Fig. 23, the wind intensifies along the coast, generating high offshore Ekman transport and divergence.

An example of temporal variation of the wind field during the period 1992- 2003, in a cross-shore transect at 20.25°S, is shown in the Figs. 24 to 27. The east-west wind stress component is negative (westward) with a few positive events along the coast (Fig. 24) and a

nearshore maximum and offshore minimum. The north-south component is positive (northward) and presents a nearshore minimum, and the maximum is located between 75°W and 83°W. The alongshore component show higher values after August 1998. This must be due to the change of satellite. Independent of that difference, it is possible to identify the seasonal cycle and some events that change the magnitude and the length of each cycle. The anomaly of these variables (Fig. 25) emphasizes these differences. The alongshore component shows a high variability, alternating between positive and negative values. Some negative anomalies in extensive periods are identified. The wind diminution alongshore is remarkable from the end of 1996 to the middle of 1997, when the wind intensifies again.

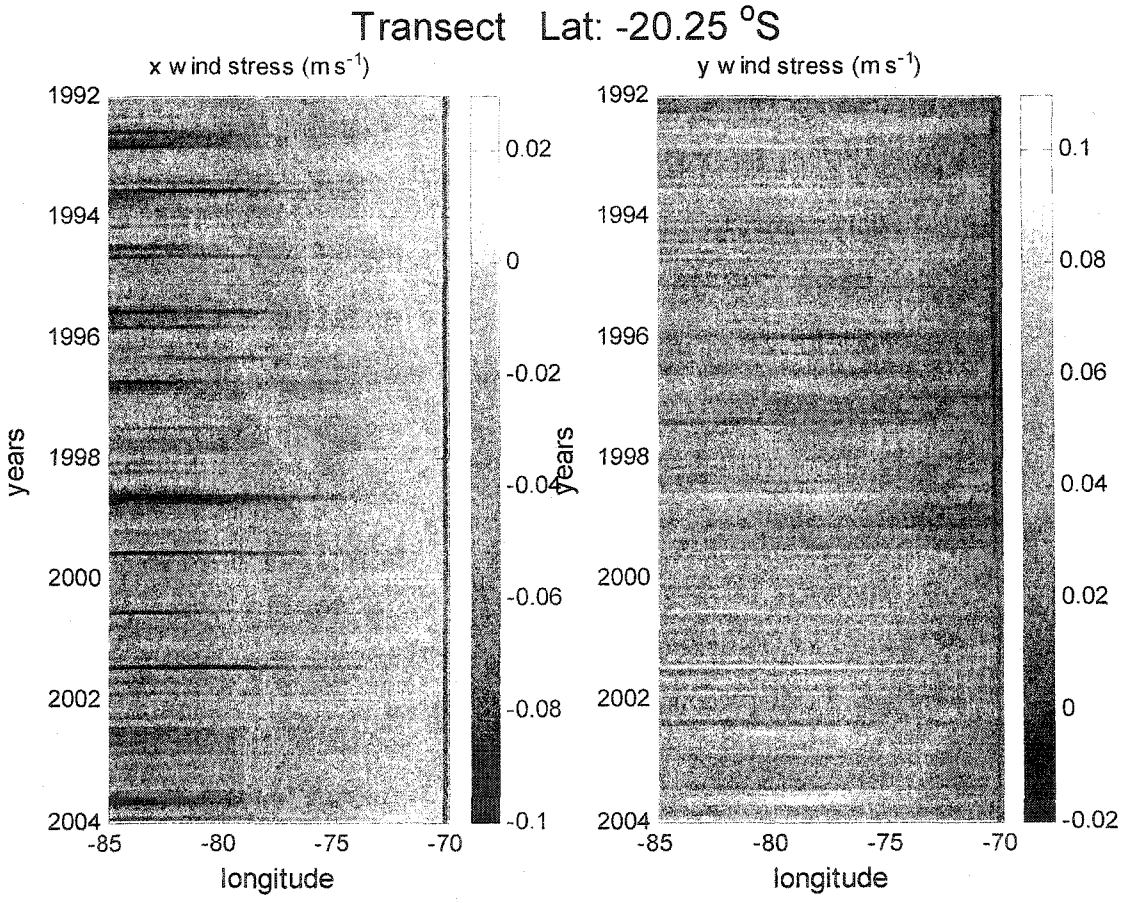

Fig. 24. Wind speed components (a) u, and (b) v derived form monthly satellite wind of ERS and QuikSCAT, cross-shore transect in 20.25°S. The black line in the right is the location of the coast.

With regard to the variability of wind divergence and to Ekman pumping (Fig. 26), the maximum is offshore with strong seasonal changes. Nearshore the values are negative (upwelling). The anomaly of these variables (Fig. 27) emphasizes the minimum divergence observed during 1995 to the middle of 1996 and an extensive period of positive divergence anomaly (convergence) from winter 1997 to winter 2000 and that continues until winter 2002. This convergence coincides with a positive Ekman pumping during the same period. A long sequence of negative Ekman pumping anomaly is observed from mid 2002 to the end of the record.

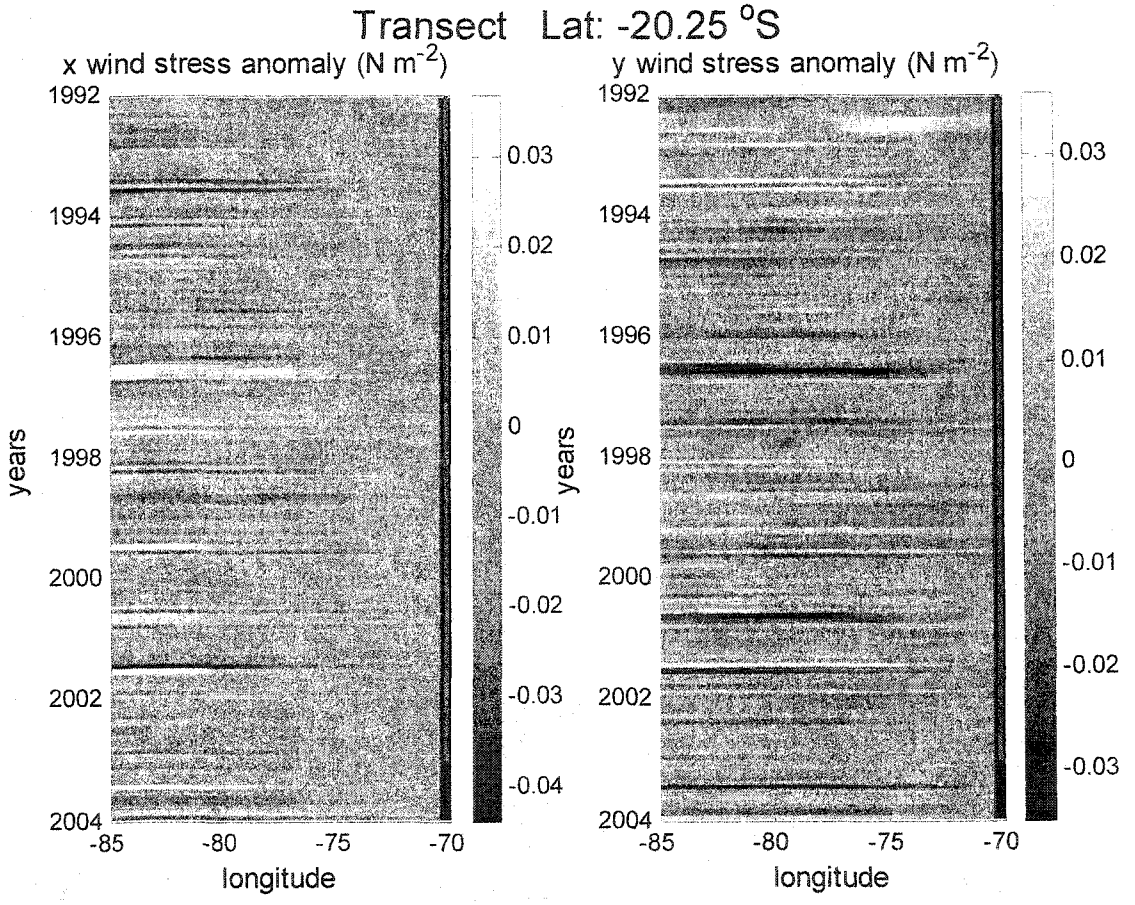

Fig. 25. Anomaly of the wind speed components (a) u , and (b) v. Monthly satellite wind of ERS and QuikSCAT, cross-shore transect in 20.25°S. The solid vertical line on the right side of the figures is the location of the coast.

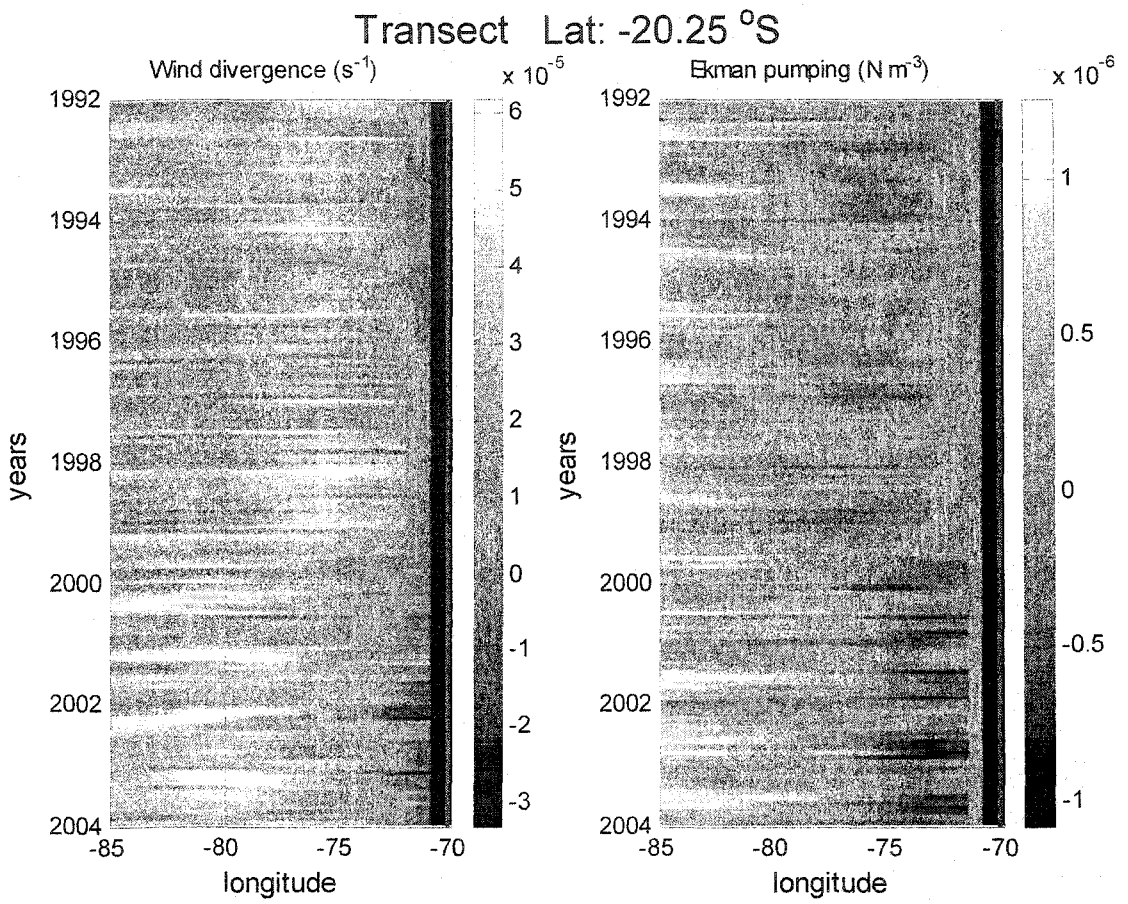

Fig. 26. ERS and QuikSCAT wind on cross-shore transect at 20.25°S. (a) Monthly wind divergence , and (b) monthly Ekman pumping . The solid vertical line on the right is the location of the coast.

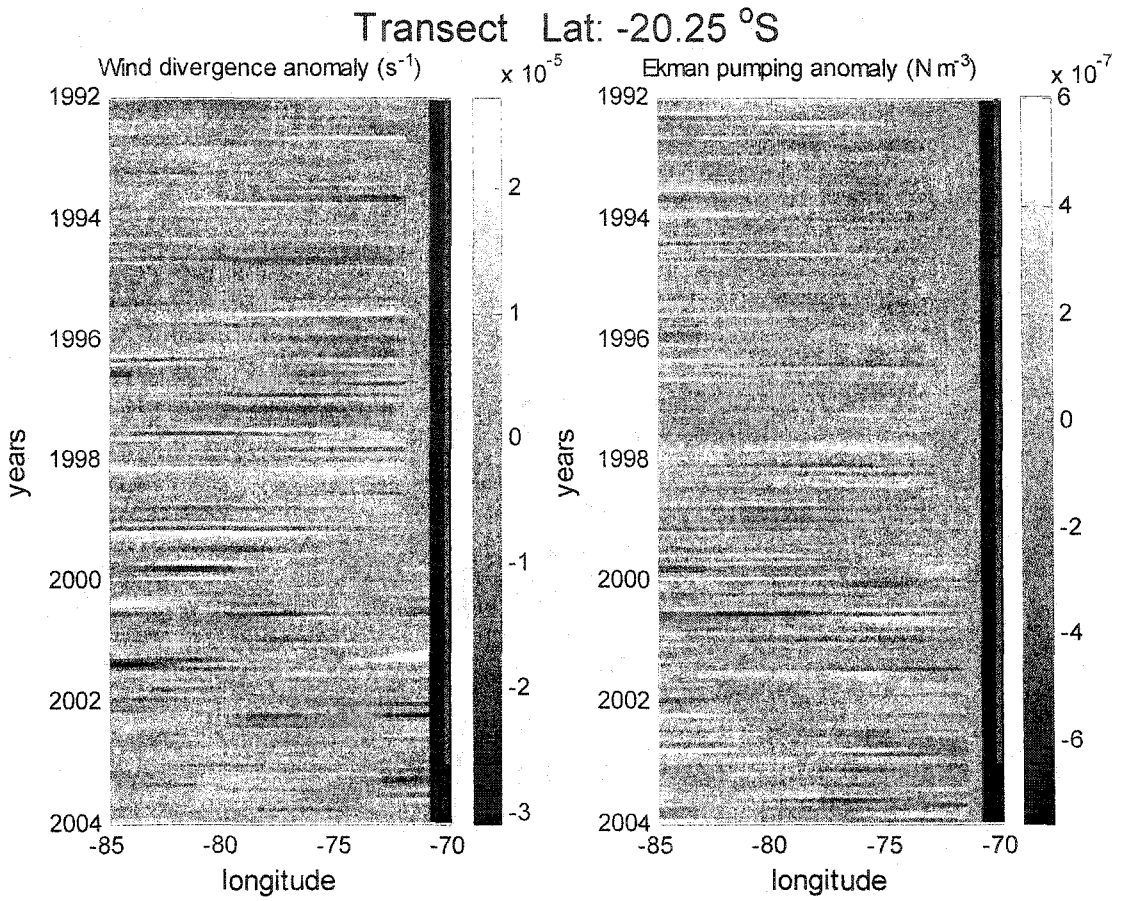

Fig. 27. ERS and QuikSCAT wind anomalies on cross-shore transect at 20.25°S (a) wind divergence anomaly, and (b) Ekman pumping anomaly. he vertical solid line on the right is the location of the coast.

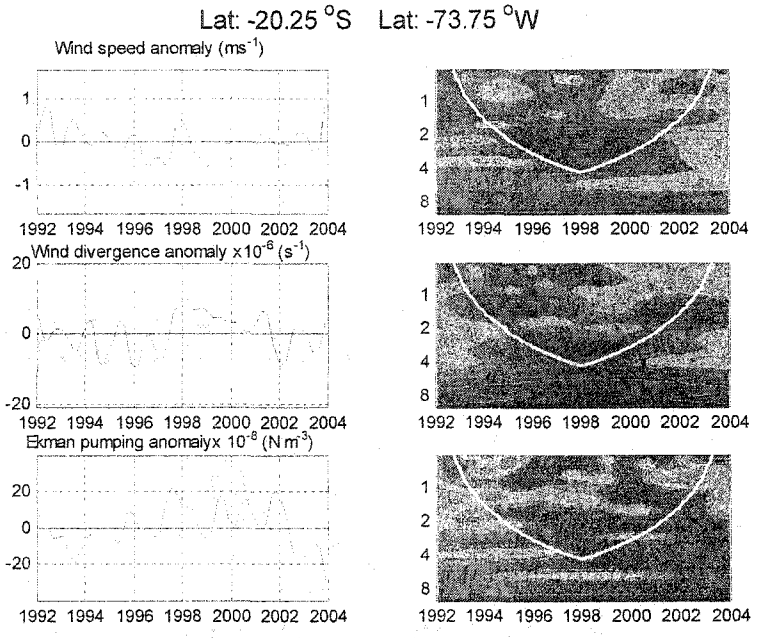

Fig. 28. Satellite derived wind divergence, wind speed, and Ekman pumping, and its frequency of variation (wavelet) in an oceanic sector (20.25°S 73.75°W).

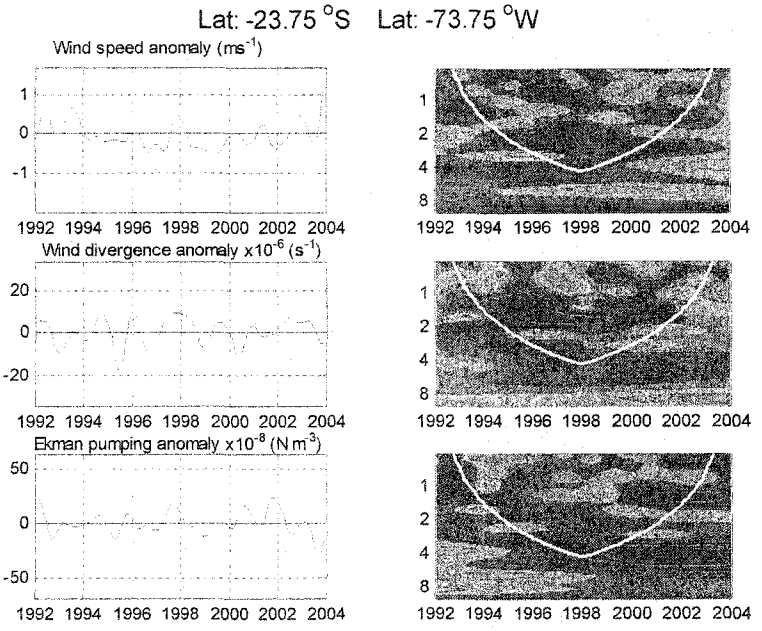

Fig. 29. Satellite derived wind divergence, wind speed, and Ekman pumping, and its frequency of variation (wavelet) in an oceanic sector (23.75°S 73.75°W).

Two time series were extracted at 73.75°W, one at latitude 20.25°S (Fig. 28) and other at 23.75°S (Fig. 29). That corresponds to the nearshore area where the climatological Ekman pumping and wind divergence are negative. The variability of each series was determined with wavelet analysis. The wind speed anomaly and the Ekman pumping anomaly are similar in both cases; however, the wind divergence anomaly presents different cycles, especially in the 1998 to 2001 period in the northern series (Fig. 28), where positive values remained. The wavelet for the wind speed anomaly show in both cases significant changes during 1997-98 with regularity of two years, and throughout all the record with a 6-year period. However, wavelet of the wind divergence and the Ekman pumping differs slightly in some periods. In any case, the observed variability is in the band of the quasi-biennial and ENSO. These graphs show that small changes of wind direction between two points produce significantly changes in the dynamics of the system that is forced by the wind divergence and the Ekman pumping and this is especially important in the study area. This also points to the sensitivity of these fields and why the wind error should be determined.

OCEANOGRAPHIC CRUISES

The temporal variability of temperature, salinity, oxygen, and density in one cross-shore transect at latitude 20.2°S is analyzed using the seasonal oceanographic cruises from 1996 to 2003. The temporal distribution at the surface (Fig. 30) was dominated by the seasonality. Showing the maximum values of temperature and salinity, and the minimum values of oxygen during the end of 1997 and the first months of 1998. In the water column, at depths of 50 to 300 m (Figs. 31 to 33) the values begin to be more homogenous and the seasonal cycle tends to disappear below 100 m. All the variables, at all levels show the disturbance due to El Niño 1997-98. The anomaly of temperature and salinity (Fig. 34) highlight the warm event of 1997-98, with a significant salinity positive anomaly, the small warm event of 2001 and the cold events of 1999 and 2000 (negative anomaly). The depth of the 15°C isotherm shows a remarkable deepening during 1997-98, but there are not changes during the 2001. The dynamic height of the sea surface relative to 500 meters (Fig. 34) shows the change of the sea level resulting from the changes in temperature and salinity. This also emphasizes the high sea level during the period 1997-98 and the seasonal cycles related to summer heating.

The biological variables were integrated alongshore and represented as a cross-shore transect (Fig. 35). The variables have in common the nearshore maximum and the offshore minimum. Chlorophyll was very low during the period 1996-97, followed by a maximum in the last half of 1999; later, show relatively high concentrations during springs and summers. The

anchovy eggs were observed in a narrow area close to the coast. They maintain a low number seasonally until the year 2001, when a significant increase was observed that was repeated in the spring of 2002 and the summer of 2003. The anchovy larvae closely followed the observed egg distribution, but the larvae extended offshore by several kilometers because of the offshore transport. This was quite evident in the spring of the 2000 and 2002. The anchovy abundance, measured by means of acoustic surveys, also shows seasonality in the abundance, with important changes in the distance from the coast and period during which the schools are present.

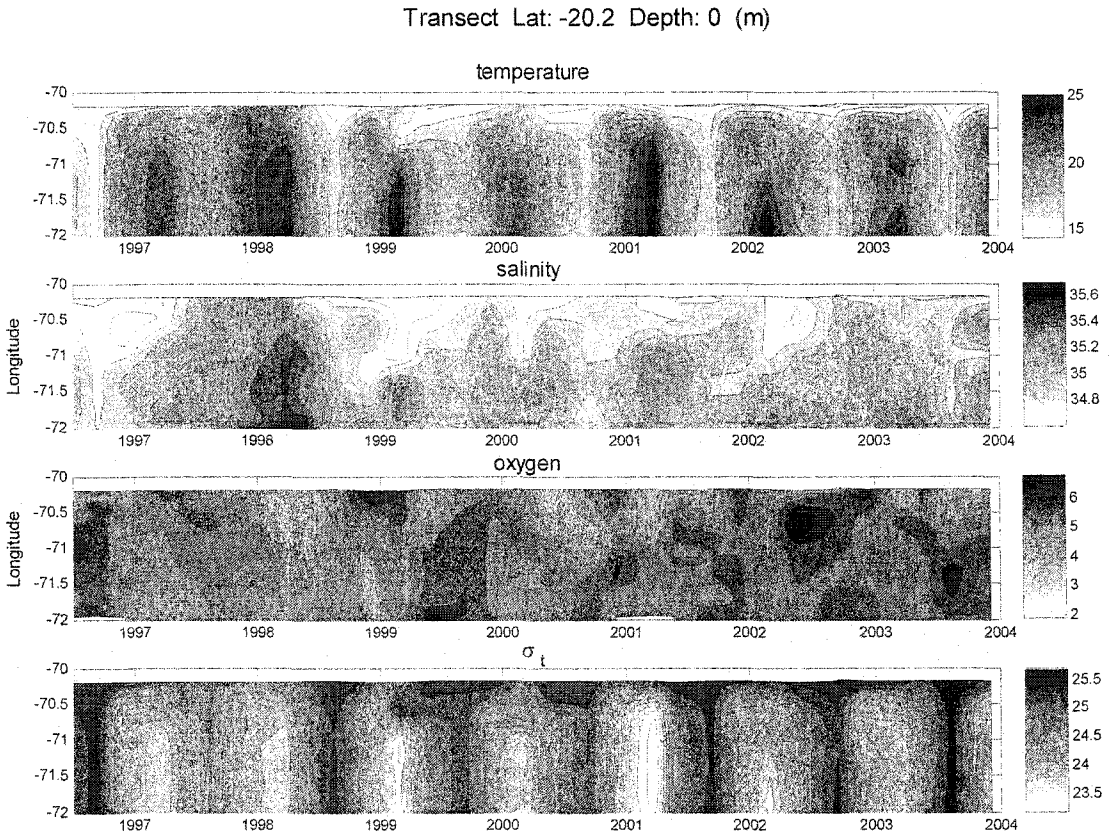

Fig. 30. Time distribution of temperature, salinity, oxygen, and density (sigma-t), at surface in a transect perpendicular to the coast at 20.2°S. Cruises between 1996 and 2003.

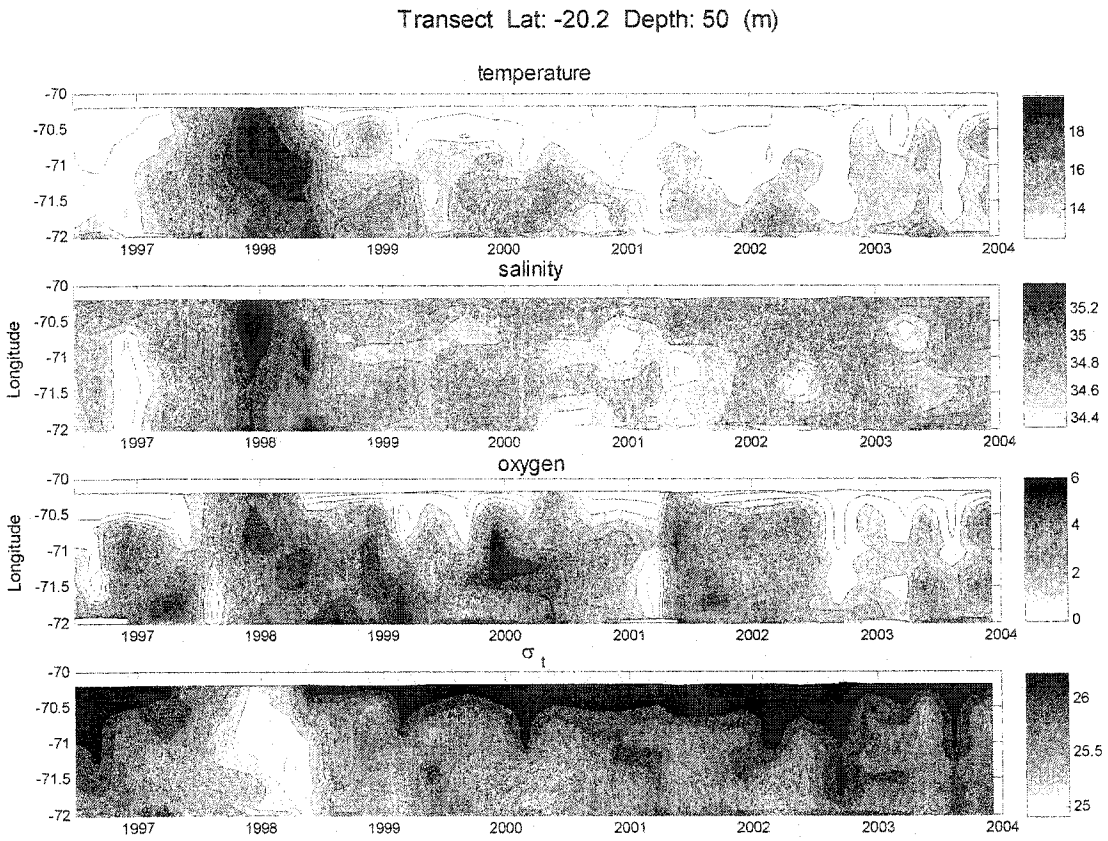

Fig. 31. Time distribution of temperature, salinity, oxygen, and density (sigma-t) at 50 m depth, in a transect perpendicular to the coast at 20.2°S. Cruises between 1996 and 2003.

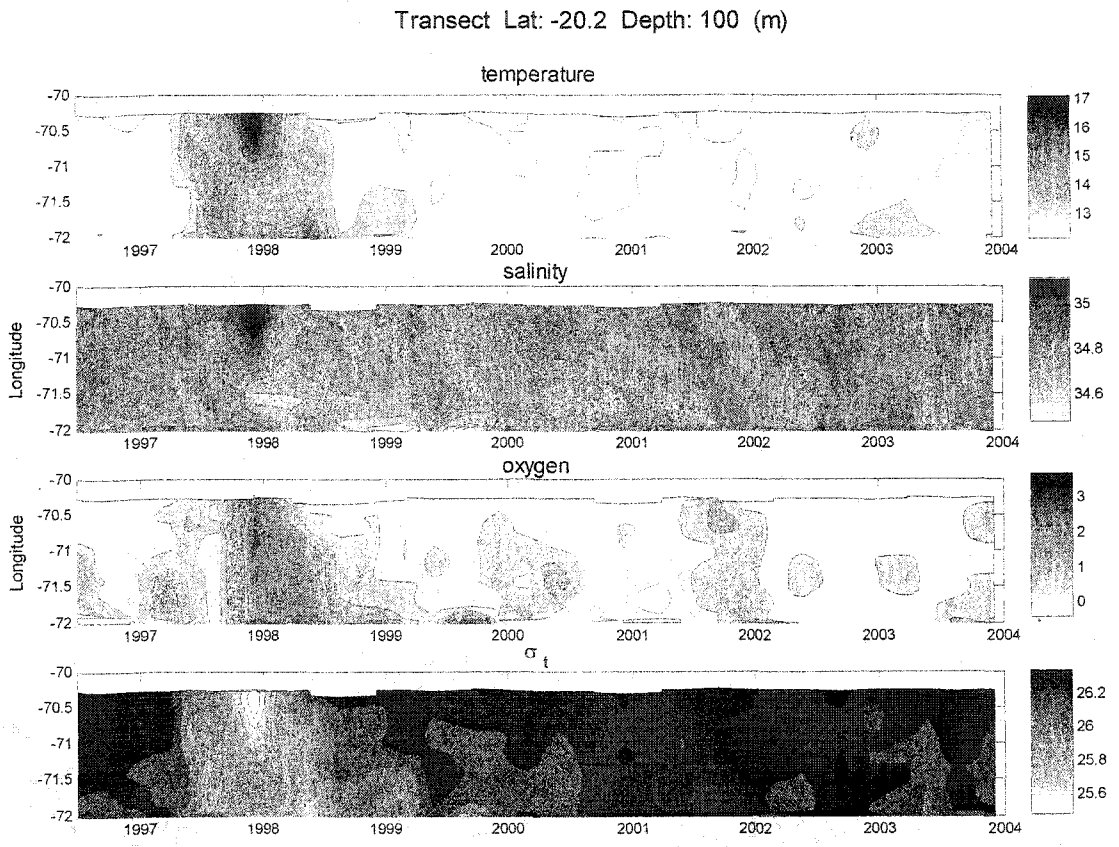

Fig. 32. Time distribution of temperature, salinity, oxygen, and density (sigma-t) at 100 m depth, in a transect perpendicular to the coast at 20.2°S. Cruises between 1996 and 2003.

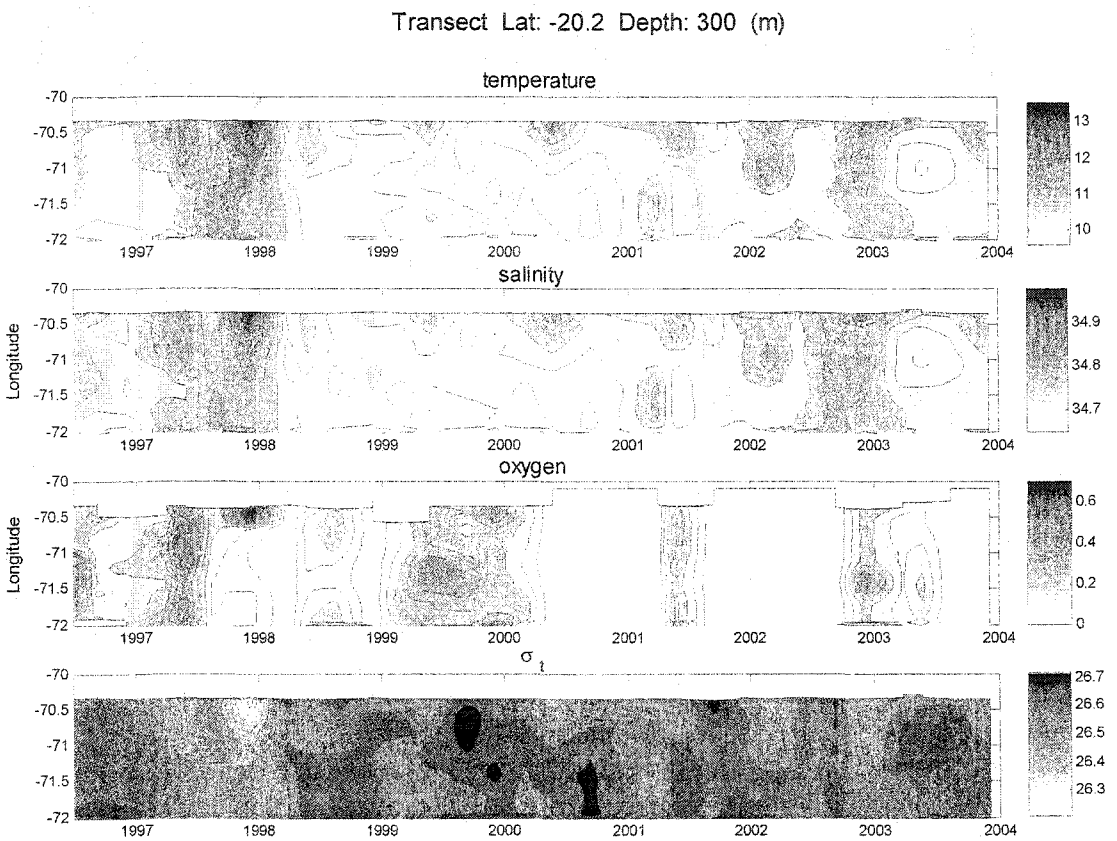

Fig. 33. Time distribution of temperature, salinity, oxygen, and density (sigma-t) to 300 m depth, in a transect perpendicular to the coast at 20.2°S. Cruises between 1996 and 2003.

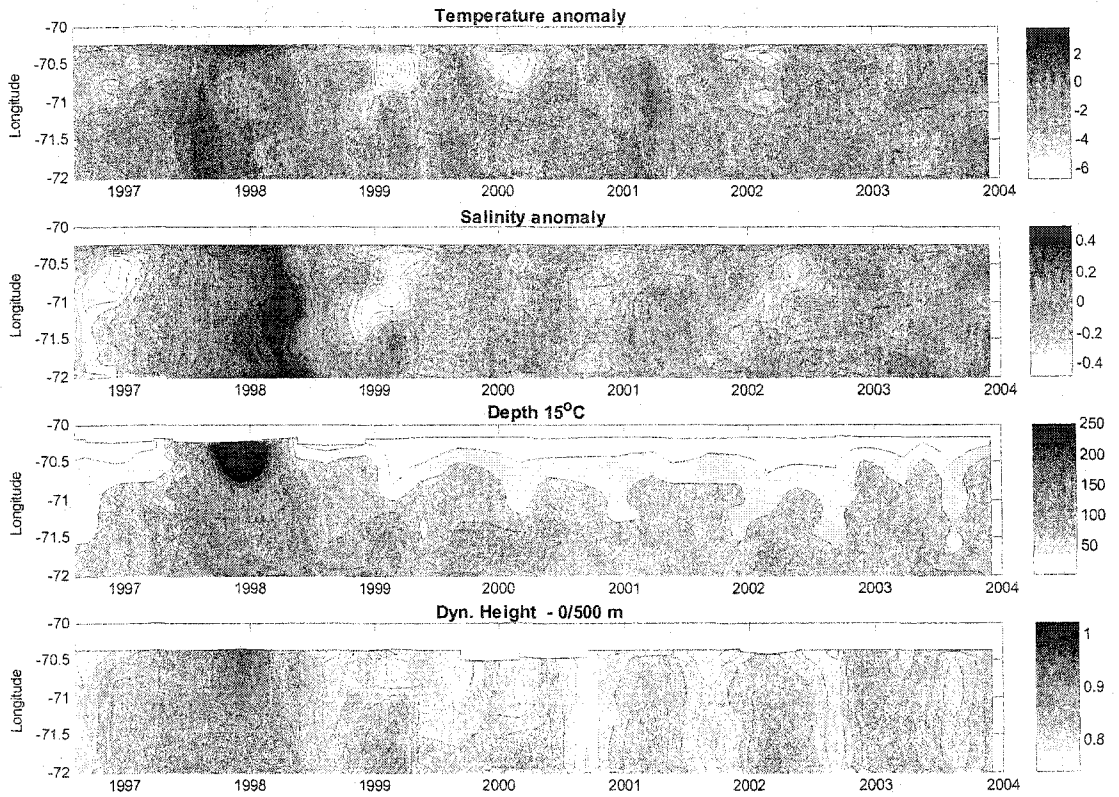

Fig. 34. Time distribution of the surface temperature and salinity anomaly, isotherm of 15°C depth and dynamic height of surface referred to 500 m, in a transect perpendicular to the coast at latitude 20.2°S. Cruises between 1996 and 2003.

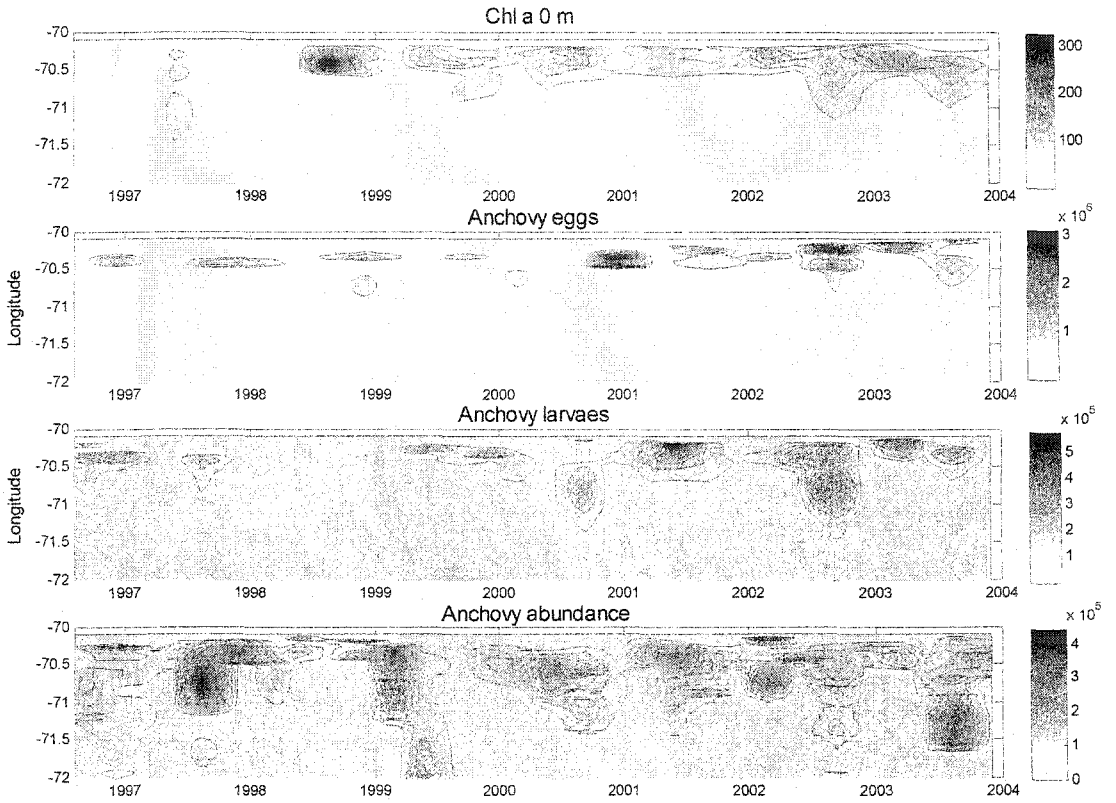

Fig. 35. Time distribution of chlorophyll, anchovy eggs, anchovy larvae and anchovy abundance (acoustic) integrated along the coast. Cruises between 1996 and 2003.

Another way to represent the previous information was by grouping the data by coastal and oceanic areas (Figs. 36 and 37). In this analysis, the seasonal cycles dominated the distribution, and clearly demonstrated the impact of the 1997-1998 El Niño on all variables. This warm event featured high temperatures and salinities in summer, a warmer winter, deepening of the isotherms to more than 150 meters, deepening of the oxygen minimum, almost total absence of chlorophyll, diminution of ichthyoplankton biomass, and changes in the accessibility of the anchovy, with a significant deepening of the schools.

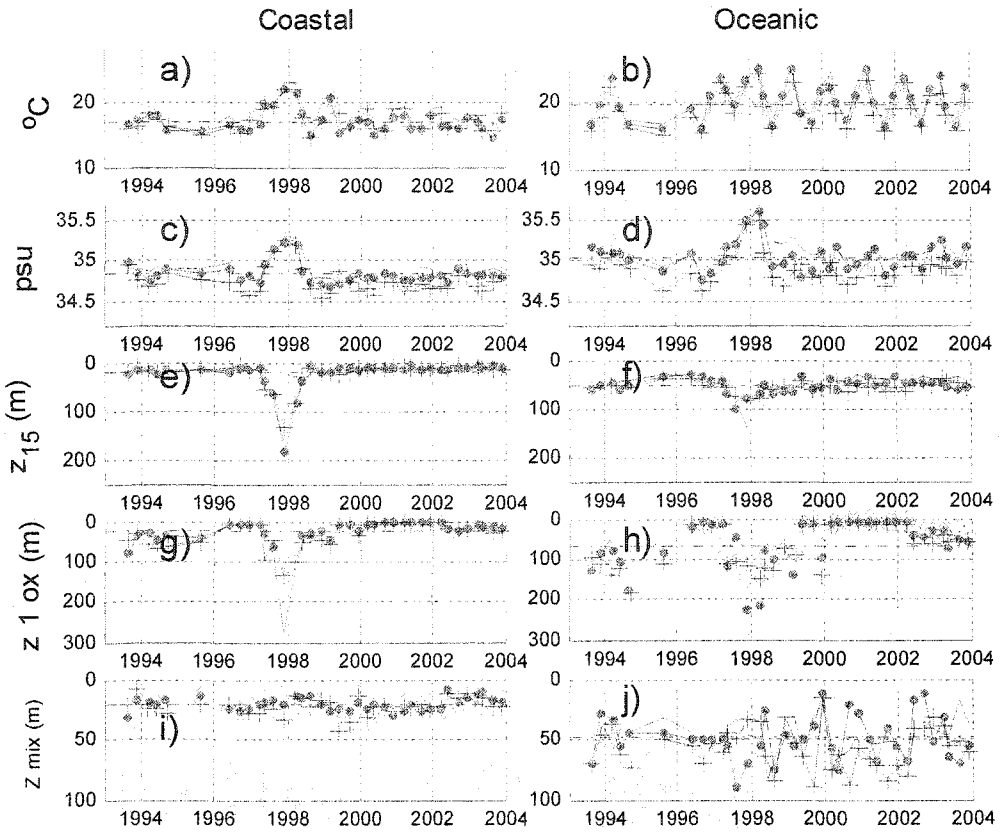

Fig. 36. Time series in a coastal area (30 km offshore) and an oceanic area (30 - 200 km offshore) off Arica, Iquique and Antofagasta. (a) and (b) SST from oceanographic cruises, (c) and (d) Sea surface salinity from cruises, (e) and (f) depth of 15°C isotherm, (g) and (h) depth of 1 ml/L oxygen isoline, and (i) and (j) mix layer depth.

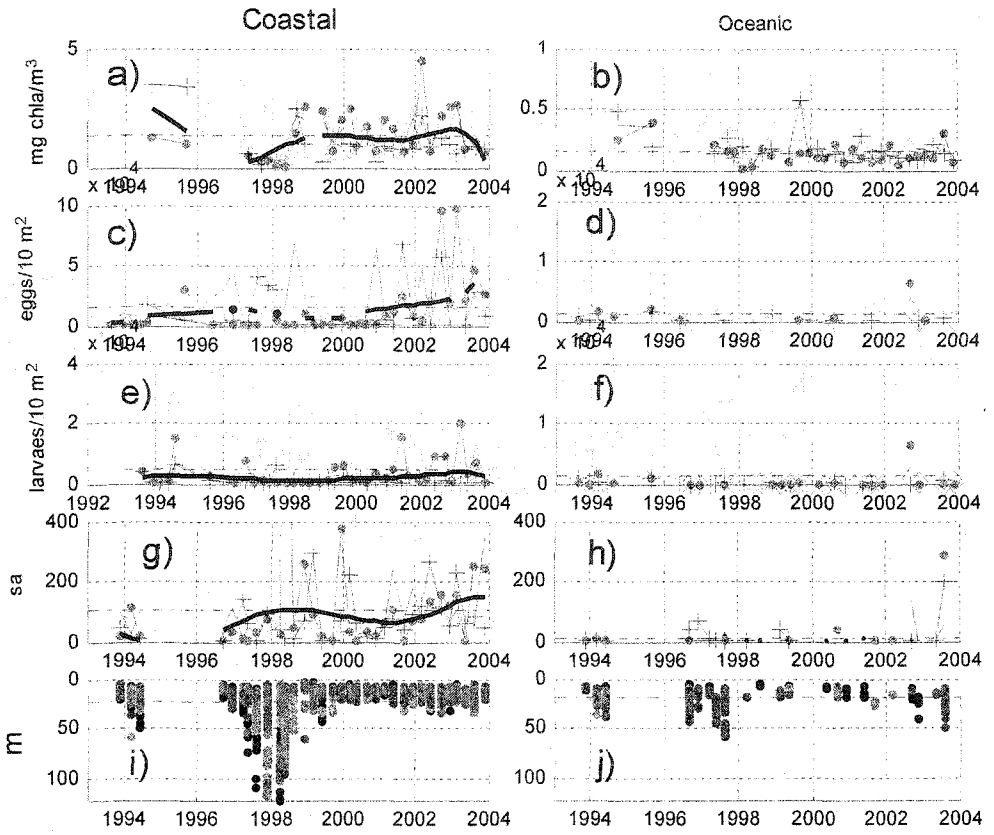

Fig. 37. Time series in a coastal area (30 km offshore) and an oceanic area (30 - 200 km offshore) off Arica, Iquique, and Antofagasta areas. (a) and (b) Surface chlorophyll, (c) and (d) Number of anchovy eggs, (e) and (f) number of anchovy larvae, (g) and h) anchovy abundance from acoustic cruises, and (i) and (j) Anchovy school depth from acoustic cruises.

DISCUSSION

The study area is located in the eastern margin of the South Pacific anticyclone, with equatorward winds throughout the year. In the oceanic area, the wind intensity is maxima in austral winter (June-September) when the Intertropical Convergence Zone (ITCZ) has moved farthest north, and minima at the end of summer (Bjerknes, 1966; Fuenzalida, 1971; Hellerman & Rosenstein, 1983; Bakun, 1985; Bakun & Parrish, 1982; Bakun & Nelson, 1991).

In opposition to the oceanic pattern, the winds at the coastal stations present the maxima in summer and the minima in winter (Fig. 4d) (Fuenzalida, 1989, Montecinos, 1991, Blanco et al., 2001). This characteristic is coincident with the strong upwelling front (~6°C) in the first 20-40 km offshore observed in summer and that disappears in winter (Blanco et al., 2001). The extension of the upwelling area is related to the Rossby ratio of deformation that in the region is 20-30 km. The difference in the wind behavior is due to the combined effect between the local-regional thermal forcing, and the large-scale atmospheric pressure field (Montecinos, 1991, Pizarro et al., 1994).

A consequence of the land-sea temperature gradient, the nearshore cyclonic wind stress curl, and the resultant upward Ekman pumping, may be significant in the austral winter off northern Chile despite weak winds there. This effect can still be seen at 30°S in spring when ERS wind maxima tend to lead coastal wind maxima (Shaffer et al., 1999). Bakun and Nelson (1991) found maximum cyclonic wind stress curl in the austral winter off Peru but not off northern and central Chile, where, however, their analysis rested upon a very sparse database.

Garreaud et al. (2002) and Rutlland et al. (2004) found that the coastal winds in the north and central part of Chile are modulated by atmospheric coastally-trapped disturbances (CDT's; e.g. coastal lows). These CDT's, that drift southwards at phase speeds of 10-20 m s^{-1} produce, on a quasi-weekly periodicity, strong alongshore gradients in the wind stress, sea-level pressure, inversion base height and cloudiness.

CDTs are characteristic along mountainous coastlines, typically west coasts, where cold upwelling results in a marine boundary layer capped by a strong low-level inversion (Garreaud et al., 2002) as in west coast of USA (Bond et al., 1996; Mass & Steenburgh, 2000) and the west coast of South Africa (Reason & Jury, 1990). These ageostrophic disturbances propagate toward higher latitudes faster than the wind, which suggests that they are not simply an advective process, but rather an internal wave-like disturbance trapped against the coast (i.e., an atmospheric Kelvin wave).

An oversimplification of the coastal wind-driven upwelling theory assumes a uniform wind blowing with the coast on its right. Nevertheless, the observations in upwelling areas show important spatial variability in different time scales. In the literature (Pringle, 2002; Pringle & Riser, 2003; Franks, 2001), four plausible mechanisms of variability and relaxation are mentioned: surface heating, wind reversals, frontal instabilities, and alongshore advection.

Integrated ecological and oceanographic studies in the coastal zone found that the frequency of upwelling-downwelling cycle dominates the community structure. Highest abundances and productive communities occur during conditions of high-frequency reversals, and lowest abundances and less productive communities are observed under low-frequency reversals (Mengue et al., 2003). Observation shows that during an upwelling wind-relaxing event the upwelling front moves onshore, transporting high concentrations of larvae shoreward (Shanks et al., 2000). These processes clearly would affect the distribution of fish larvae.

Results from modeling studies suggest that mixed layer processes can be favorable or unfavorable to larval survival depending on the turbulence intensity (Davis et al., 1991). Periods with moderate winds and a shallow mixed layer resulted in food concentrations, growth at age and mortality rates that were more favorable to larval survival than during periods when strong winds were accompanied by a deep mixed layer (Bailey et al., 1995).

Without a doubt, the above mentioned processes are important for the productivity of upwelling systems, but they correspond to high frequency processes that escape the objective of this thesis. However they need to be mentioned due to their importance and because they may partly explain the high productivity and the larval transport in the study area.

The satellite wind data is particularly useful in many coastal areas of the world's oceans such as off Peru and Chile that currently are deficient in direct wind measurements. However, the nearshore wind data must be used carefully in light wind conditions because the satellite decreases the ability to determine wind direction (Pickett et al., 2003). Also the wind structure cross-shore has significant changes at scales less than 10 km (Capet et al., 2004) that can not be resolved with the satellite resolution (QuikSCAT – 25 km).

Pickett et al. (2004) found that satellite-buoy wind speed differences in the nearshore were about 30% larger, and wind direction differences were about 70% larger than at offshore buoys. These differences were mainly due to the complexity of the coastal winds. In addition, the sensor design specifications of satellite and buoys must be considered (satellite: wind speed +/- 2 ms^{-1}, and direction +/- 20 degrees, buoys: 1 ms^{-1} and 10 degrees). Also the data can be biased by the gravity wave direction (Rieder et al., 1994; Pickett et al., 2003). Despite all these limitations,

and considering the results obtained in the data validation, the correlations between satellites-wind and the buoys-wind are remarkable.

On the other hand, geostrophic-derived winds, another source of wind data, are reasonably accurate along the North America's west coast. Off South America, however, geostrophic-derived winds had large errors, especially at lower latitudes (Pickett et al., 2004). Possible explanations for this poor performance are the high coastal mountains (>2,000 m) that can produce both nearshore bands of strong wind-stress and wind-stress curl (Dorman et al., 1995; Dorman et al., 2000) as well as large surface pressure changes (Winant et al., 1988). Also, the mentioned CDTs could play an important role in this complex land-ocean-atmosphere system.

According Pickett et al. (2004), "upwelling indices based on geostrophic-derived winds agreed with those based on satellite-measured winds at 85% of North American and 65% of South American sites. Upwelling indices based on model-derived winds, on the other hand, agreed at 100% of North American sites and 80% of South American sites. Although model-based upwelling indices represented an improvement, they were not accurate in all locations. Off South America where the rugged coast veers sharply eastward near the Peru-Chile border, model-based upwelling estimates are poor".

The spatial variation of wind stress over the ocean causes surface divergence of horizontal flow, which in turn gives rise to vertical mass flux through Ekman pumping (W_E). Since it is directly proportional to wind stress, Ekman pumping in the area has significant spatial and temporal variability (Figs. 20 and 26). Although the magnitude of this offshore vertical flow is quite small (i.e., order of m day^{-1} to cm day^{-1}) compared to the horizontal flow, it can have significant effect on mixed layer processes and the SST, because of its small length scale (i.e., comparable to mixed layer depth).

The study area shows an area with a negative W_E (Fig. 20), indicating a net outflow of surface water in response to Ekman pumping. For mass conservation, this may give rise to inflow at the lower levels. This offshore process presents an important seasonal and interannual variability, being affected principally by ENSO events (Figs. 22, 23, 25 and 27).

Figure 38 shows the alongshore satellite-wind speed in a cross-shore transect at 20.25°S for the climatologic summer and winter mean, a low intensity wind during the El Niño onset (May 1997), and for the intense wind period during La Niña (February 2000). The data from the coastal station of Iquique corresponding to each period was included. The thermal acceleration produced in summer over the coastal-wind induces a coastal divergence and a negative Ekman pumping in a narrow area along the coast. These processes increase the upwelling produced by the Ekman transport. The wind change takes place over an increasingly small region, as the

resolution increases, the divergence and the wind curl increase proportionally. The magnitude of this divergence decreased during El Niño and increased during La Niña. Pickett and Paduan (2003) and Enriquez and Friehe (1995) argued that the upward Ekman pumping associated with a large curl is comparable in magnitude with the effect of Ekman coastal divergence, and that the upwelling might be independent of the separate contributions since increased Ekman pumping would compensate for any decrease in coastal divergence.

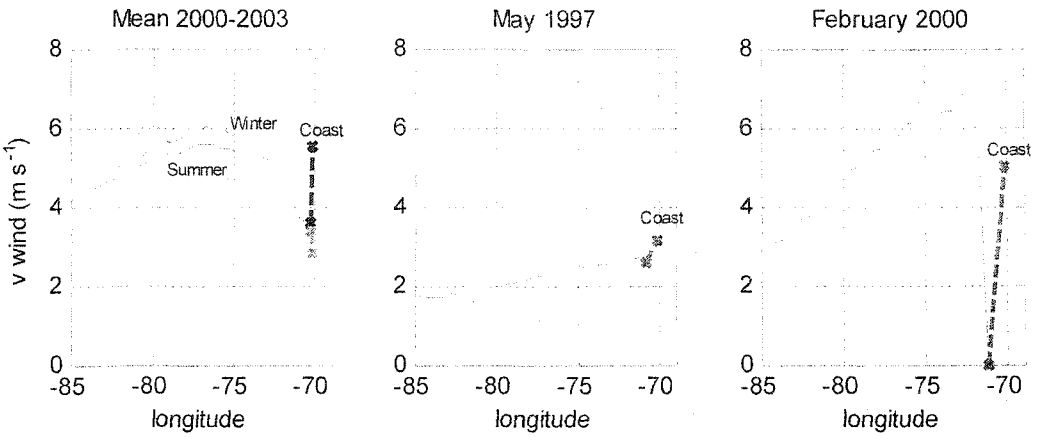

Fig. 38. Along shore wind speed transect at 20.25°S extending from the coast offshore: (a) Climatologic alongshore winds for summer and winter, (b) data during onset of El Niño – may 1997, (c) data during intense La Niña period – February 2000. Thin line is QuikSCAT satellite wind and the thick line is the connection between coastal wind (x) and nearshore satellite wind.

The combined effect of the winds that decrease from the coast to a minimum at the upwelling front and increase again offshore, produces a convergence further offshore of the upwelling front. Since the wind variability is on the scale of days, this convergence could be the origin of the mesoscale eddies that are observed in the area (Narvaez, 2000). Another important characteristic, that needs further study, is the offshore divergence produced in the area of the offshore maximum values of the alongshore wind stress, that produces a negative Ekman pumping that could be responsible for a rise of the thermocline in the area.

The competition between coastal divergence and offshore Ekman pumping explains how the nearshore wind profile affects the upwelling circulation. Also, the wind structure close to the coast plays an important role in setting the alongshore current structure (Marchesiello et al., 2003). Equatorward winds at the coast force a surface equatorward jet and poleward undercurrent. However, the depth-averaged poleward currents are related to positive wind curl (negative Ekman pumping) through Sverdrup balance (the eddy Reynolds stress further acts to redistribute the wind-curl input). Capet et al. (2004) found that large positive wind curl and weak coastal wind favor poleward currents.

The depth of the mixing layer (MLD) is influenced mainly by the wind stress, and advection processes. In general, there is a good correlation between negative W_E and shallow MLD. In addition, the depth of the Ekman layer is totally coherent with MLD, as can be observed in Fig.s 20 and 36i-36j.

Schwing and Mendelssohn (1997), using state-space models that separate the seasonal component, demonstrate the importance of considering changes in seasonal patterns independently from changes in the long-term climate trend. Here the results obtained by STL method show a clear separation of the seasonal signal from the long-term trend in all the series analyzed.

Bakun (1990) using data from different subtropical systems during the period 1945 to 1985 found an intensification of the upwelling and postulate that under the scenario of global warming stronger equatorward wind stress will increase coastal upwelling along eastern ocean boundaries. Similarly Schwing and Mendelssohn (1997) using long time series ending in 1992 from the west coast of USA, found a similar trend, confirming Bakun's results. The data used here include information up to 2003. The trend obtained until early 90's agree with Bakun's results and shows an upwelling intensification. Nevertheless, the trend change during the last decade, and the actual long-term scenario is a reduction in the upwelling and the number of Lasker events increase.

Tourre et al. (2001) determined the spectrum for SST and the SLP anomalies in the Indo-Pacific Ocean for the last 100 years, finding significant peaks for biennial (2.2 and 2.8 year) signals, interannual (3.5, 5.4, and 7 year) signals, and a decadal (11 year) signal (Allan, 2000, White & Cayan, 2000). These quasiperiodic signals are similar to those observed by Mann and Park (1996) and Lau and Weng (1995) in SST and SLP anomalies over the Northern Hemisphere during the past century, and coincident with the observed in this study (Fig. 10 and 11). The EOF analysis of the time series in the study area determines that the interdecadal and quasi-biennial signals (mode 1) explain a 64% of the variance, and ENSO explain 34% of the variance (mode 2).

The ENSO effects in the region are forced remotely by teleconnection, planetary waves, and advection. The OLR that represents the activity of the Madden and Julian Oscillation (MJO) showed a high coherence with the SST and the wind at the coastal stations in the bands of biennial, ENSO and, with a lag of between 3 to 4 months, a similar pattern was found for the SOI. A measurement of the process's intensity alongshore was estimated by the difference of atmospheric pressure between Easter Island and Antofagasta. This standardized difference was defined here as Humbold Current Index (HCI). This index presents variations in decadal scale mainly, showing a high coherence in variations of 5 years and in phase with the SST.

Studies from the western coast of North America (Lluch-Cota et al., 2001) and from the western coast of South America (Montecinos et al., 2003) found that the ENSO-related SST variability decreases poleward from subtropical latitudes, while interdecadal variability increases from subtropics to midlatitudes.

White et al. (2003) used a model of a delayed oscillator mode (DAO) to explain the origin of the biennial, interannual, and decadal variations (McCreary, 1983; Zebiak & Cane, 1987; Schopf & Suarez, 1988; Graham & White, 1988). In the DAO mode, the incidence of the off-equatorial Rossby waves on the western boundary are reflected as equatorial Kelvin waves, the latter appearing raises the depth of the pycnocline in the eastern equatorial Pacific Ocean (Battisti, 1988). This sequence of cause and effect produces a delayed negative feedback that cools the high SST anomalies in the eastern equatorial Pacific Ocean (White et al., 1985, 1986, 1987, Pazan et al., 1986, Philander, 1990)

Maruyama (1997), analyzing the data at three stations over the Indian Ocean, showed that the intensities of Kelvin waves and mixed Rossby gravity waves had a phase relationship with the Quasi Biennial Oscillation (QBO). Maruyama and Tsuneoka (1988) noted that the rapid descent of the QBO westerly was accompanied with the El Nino. The El Nino event enhanced Kelvin wave activities, and it maybe possible to explain the rapid westerly wind descent. Rasmusson et al. (1990) also found that the QBO is a fundamental component of ENSO variability, giving a degree of regularity in the ENSO cycle; nevertheless, they say that the relationship between the surface biennial mode and the stratospheric QBO is unclear.

Considering the previous observations, it is possible to assume that away from the equator, the signal in the band of two years induced by the QBO in the equatorial area, is associated remotely to the system through the ocean and atmosphere coastal trapped waves that are modulated according to the DAO mode.

The ENSO events can dramatically affect the pelagic fish populations, but, although ENSO is commonly thought of having long-lasting detrimental effects on the anchovy, it turns

out that ENSO causes short-term perturbations in the dynamics of anchovy from which it seems to recover rather quickly within one or two years during the following La Nina phases. The fishing activity is affected by the long–term variability (Yañez et al., 2001). Alheit and Niquen (2004) mentions the anchovy migrations as the primary factor explaining the quick recovery, nevertheless the evidence presented here showing the deepening of the schools, to depths without precedent, suggest that this mechanism could be more important than migration.

Over the past two decades, earlier beliefs in the essential stability of marine ecosystems have been largely replaced by a growing appreciation of the importance of large-amplitude and low frequency variability occurring in many regions of the world's oceans. For example, Roemmich and McGowan (1995) reported a 70% decrease in zooplankton biomass in the California Current since the 1950s, along with corresponding drastic declines in certain seabird species. A sharp 60%-70% decline in zooplankton biomass off Peru in the mid-1970s, following the collapse of the anchovy population, was also reported (Carrasco & Lozano, 1989; Loeb & Rojas, 1988; Alheit & Bernal, 1993).

This mode of low frequency variability seems to often take on the appearance of periods of relative stability over time scales of one to several decades which are interspersed by comparatively sudden "regime shifts".

Irrefutable evidence of the biological changes in the Humboldt Current before 1976 is reported by Loeb and Rojas (1988). They studied the interannual variation, composition, and abundance of ichthyoplankton of northern Chile from 1964 to 1983 and observed a significant change in the relative abundance of mesopelagic species larvae between 1969 and 1970. The importance of this observation is that the abundance of mesopelagic species is not influenced directly by the fisheries activities; therefore, it could be a good indicator of the environmental changes.

In the Humboldt Current system, decadal period switches in dominance between sardine and anchovy populations have occurred during the last century (Fig.1) (Alheit & Niquen 2004; Chaves et al., 2003; Schwartzlose et al., 1999; Yañez et al., 2001). It is also apparent from the analysis of fish scales in sediments that species alternations have occurred during the past centuries, i.e. prior to the industrial fishing and other anthropogenic impacts. Moreover, it has been demonstrated that populations of sardine in different parts of the Pacific (off Chile/Peru, California/Mexico, and Japan) have undergone synchronous fluctuations this century. In the Benguela ecosystem, there have been corresponding fluctuations in sardine abundance, although these appear to be out of phase with those in the Pacific (Shannon and O'Toole 1999).

During the last century, five regime shifts has been reported for the North Pacific Ocean: 1925, 1950, 1976, and 1998 (Hare &Mantua, 2000; Chavez et al., 2003; Alheit & Niquen, 2004). From the Fig. 9 and Table 4 the regime shift found off the northern Chile and probably extensive to all the Humbold Current system, are coincident with the period reported for the North Pacific. A regime shift was reported by Mantua (2000) during 1989. This shift was questioned by Rudnick and Davis (2003) due the methodology used by Mantua (2000). In the analysis made here, some variables of marine origin shown a variation during 1989. Nevertheless, the atmospheric series do not show any change. According to Rudnick and Davis (2003) evidence exists for the interdependence of the atmosphere, ocean, and biota on a variety of time scales, that could explain this variations. Consequently, the changes observed in northern Chile during 1989 do not constitute a regime shift.

CONCLUSIONS

This thesis use satellite wind data for to determine the spatial variability of the wind field. Satellite derived winds are an important source of data. Especially the data from QuikSCAT satellite due its high resolution, offering the advantage of real-time coverage of all the world's coastal zones. Offshore, the satellite-measured wind correlation with in situ measured wind is excellent. Nevertheless, nearshore the errors are larger and need to be validated before used in study. This is especially the case were the wind is weak and the coast is mountainous.

The seasonal cycle in the study area is a balance of the upwelling wind cycle and the heating and cooling cycle and their amplitude is modulated with decadal periodicity.

The wind field in the study area had a wind stress with a minimum between two maximums, which were located at 15 and 30°S. The effect of the curvature as well as the height of mountains near the coast produce a very unique system, where the wind is forced thermally and reaches a maximum in summer and a minimum in winter, opposed to the oceanic pattern. In addition, in spring and summer the wind along the coast is accelerated by changes in the cross-shelf pressure gradient, producing an intense divergence close to the coast. In the nearshore, the wind remains at a low intensity and increases offshore. The combined effect of both processes produces a convergence outside of the upwelling front. Considering the variability of the wind in scale of days, this convergence could be the origin of the mesoscale eddies that are observed in the zone. Important changes of this pattern are observed during ENSO events.

Spectral analysis presents 4 bands of variability: biennial or quasi biennial (2-3 years, ENSO (3 to 8 years), decadal (9-12 years) and interdecadal (13 to 25 years). The origin of quasi-biennial variability could be explained by means of the Delayed Oscillator Model. The interdecadal variability was obtained by the trend of the STL analysis, the change of sign represent a regime change (Regime shift). It is possible to see three regimes, one cold, before 1976, another warm between 1976 and 1998 and one after 1998 beginning with a cold phase, similar regimes were defined for the North Pacific Ocean. In addition, these changes correspond with the alternation between anchovy and sardine populations in the Chile-Peru system. In variables that represent the ocean, a change or alteration is also registered during the year 1989, but that is not observed in the meteorological time series. The trend shown by the different variables along the coast, in the last years, indicates a diminution of upwelling, an increase of the Lasker events (calm), a diminution of the temperature, the sea level, and the atmospheric pressure.

The ENSO effects in the region are forced remotely by planetary waves, and advection. The OLR that represents the activity of the Madden and Julian Oscillation (MJO) showed a high coherence with the SST and the wind at the coastal stations in the bands of biennial, ENSO and, with a lag of between 3 to 4 months, a similar pattern was found for the SOI. A measurement of the processes intensity along the coast was estimated by the atmospheric pressure differential between Easter Island and Antofagasta. This standardized difference was defined here as Humbold Current Index (HCI). This index presents variations in decadal scale mainly, showing a high coherence, in phase with the SST, in the variations of 5 years. The variability of the seasonal cycle is represented principally with a different variance in the decadal scale for each season. The EOF analysis shows that the first mode corresponds to the inter-decadal and quasi-biennial changes explaining 64% of variance and the second mode correspond to ENSO explaining 34% of the variance.

From the analysis made here it is possible to conclude that the STL is a robust and effective method to estimate the trend and the seasonality.

El Niño produced changes in the density, distribution, and depth of the anchoveta schools, with migrations of the north and south stock towards the south, making them more vulnerable to capture. Nevertheless, it was demonstrated that the deepening of some schools in the coastal area, moves them deeper than fishing nets and would explain the populations' recovery rapidly after disappearance of the anomaly.

Many questions remain, but answering them will require more and longer time series, new studies, and new information. It is necessary to reconsider the meaning of regime shift – clarify definition, periods of change and include biological series along of the South America coast. Were the anchovy and sardine cycles modified by overfishing in the last century? Which is the relative importance of fish migration and fish deepening processes during EN?

Other topics that need to be studied are the relative importance of the Ekman transport, wind divergence, and Ekman pumping in the upwelling processes, in both temporal scales of high and low frequency. And finally, it is necessary to study the plausible mechanisms for upwelling variability and relaxation, like surface heating, the wind reversals, the frontal instabilities, and the alongshore variations in cross-shore advection.

Additionally, it is important to determine the error of the satellite wind field in the nearshore using coastal buoys, flights, etc.

REFERENCES

Alheit, J. & Bernal, P. (1993). Effects of physical and biological changes on the biomass yield of the Humboldt Current Ecosystem. In K. Sherman, L. Alexander et al. (Eds.) *Large Marine Ecosystems: Stress, Mitigation and Sustainability.* (pp. 53-68). Washington, DC: AAA Press.

Alheit, J. & Niquen, M. (2004). Regime shifts in the Humboldt Current ecosystem. *Progress In Oceanography, 60*, 201-222.

Allan, R. J. (2000). ENSO and climatic variability in the last 150 years. In H. F. Diaz & V. Markgraf (Eds.) *El Nino and the Southern Oscillation: Multiscale Variability, Global and Regional Impacts* (pp. 3-55). New York: Cambridge Univ. Press.

Arakawa, A. & Lamb, ..R. (1977). *Methods of Computational Physics*. Academic Press.

Bailey, K. M., Canino, M. F., Napp, J. M., Spring, S. M. & Brown, A. L. (1995). Contrasting years of prey levels, feeding conditions, and mortality of larval walleye pollock Theragra chalcogramma in the western Gulf of Alaska. *Marine Ecology Progress Series, 119*, 11-23.

Bakun, A. & Nelson, C. S. (1991). The seasonal cycle of wind-stress curl in subtropical eastern boundary current regions. *Journal of Physical Oceanography, 21*, 1815-1834.

Bakun, A. & Parrish, R. H. (1982). Turbulence, transport, and pelagic fish in the California and Peru Current systems. *Calcofi Rep., 23*, 99-112.

Bakun, A. (1985). Comparative estudies and the recruitment problem: Searching for generalizations. *CalCOFI Rep., XXVI.*

Bakun, A. (1990). Global climate change and intensification of coastal ocean upwelling. *Science*, 247, 198-201.

Bakun, A. (1996). Patterns in the ocean. Ocean processes and marine population dynamics. *California Sea Grant/cib, .*

Barber, R. (1988). The ocean basin ecosystem. In J. J. Alberts & L. R. Pomeroy (Eds.) *Concepts of Ecosystem Ecology* (pp. 166-188). New York: Springer-Verlag.

Battisti, D. S. (1988). Interannual variability in the tropical atmosphere-ocean models. In M. E. Schlesinger (Ed.), *Climate Ocean Dynamics* Mass.: Kluwer Acad., Norwell.

Behrenfeld, M. J., Randerson, J. T., McClain, C. R., Feldman, G. C., Los, S. O., Tucker, C. J., Falkowski, P. G., Field, C. B., Wayne, R. F., Esaias, E., Kolber, D. D. & Pollack, N. H. (2001). Biospheric Primary Production During an ENSO Transition. *Science, 291*, 2594-2597.

Bjerknes, J. (1966). Possible Response of the Atmospheric Hadley Circulation to Ecuatorial Anomalies of Ocean Temperature. *Tellus, 18*, 820-829.

Bjornsson, H. & Venegas, S.A. (1997). *A Manual for EOF and SVD Analysis of Climatic Data.* Montréal, Québec: McGill University.

Blackman, R.B. & Tukey, J.W. (1958). *The Measurement of Poeer Spectra From the Point of View of Communication Engineering*. New York: Dove, Mineola.

Blanco, J. L., Carr, M.-E., Thomas, A. C. & Strub, P. T. (2002). Hydrographic conditions off northern Chile during the 1996-1998 La Nina and El Nino events. *Journal of Geophysical Research, 107*, 3-1-3-19.

Blanco, J. L., Thomas, A. C., Carr, M.-E. & Strub, P. T. (2001). Seasonal climatology of hydrographic conditions in the upwelling region off northern Chile. *Journal of Geophysical Research, 106*, 11451-11467.

Bograd, S., Chereskin, T. K. & Roemmich, D. (2001). Transport of mass, heat, salt, and nutrients in the southern California Current System: Annual cycle and interannual variability. *Journal of Geophysical Research, 106*, 9255-9275.

Bond, N. A., Mass, C. & Overland, J. (1996). Coastally trapped southerly transitions along the U.S. west coast during the warm season. Part I: Climatology and temporal evolution. *Mon. Wea. Rev.*, 124, 430–445.

Bond, N. A., Verland, J. E., Spillane, M. & Stabeno, P. J. (2003). Recent shifts in the state of the North Pacific. *Geophysical Research Letters, 30*, 2183-doi:10.1029/2003GL01.

Capet, X. J., Marchesiello, P. & McWilliams, J. C. (2004). Upwelling response to coastal wind profiles. *Geophysical Research Letters, 31*, 3311-doi:10.1029/2004GL02.

Carr, M.-E., Strub, P. T. , Thomas, A. C. & Blanco, J. L. (2002). Evolution of 1996–1999 La Nina and El Nino conditions off the western coast of South America: A remote sensing perspective. *Journal of Geophysical Research, 107*, , 3236.

Carrasco, S. & Lozano, O. (1989). *Seasonal and long-term variations of zooplankton volumes in the Peruvian Sea, 1964-1987.* Callao, Peru:

Chavez, F. P., Ryan, J., Lluch-Cota, S. E. & Ñiquen, M. (2003). From Anchovies to Sardines and Back: Multidecadal Change in the Pacific Ocean. *Science, 299*, 217-221.

Cleveland, R., Cleveland, W., McRae, J. & Terpenning, I. (1990). Seasonal-trend decomposition procedures based on Loess. *Journal of Official Statistics, 6*, 3-73.

Cook, E. R., Meko, D. & Stockton, .. W. (1997). A new assessment of possible solar and lunar forcing of the bidecadal drought rhythm in the western United States. *Journal of Climate, 10*, 1343-1356.

Davis, C. S., Flierl, G. R., Wiebe, P. H. & Franks, P. J. S. (1991). Micro-patchiness, turbulence and recruitment in plankton. *Journal of Marine Research. 49*, 109-151.

Denman, K., Hofmann, E. E. & Marchant, H. (1996). Marine biotic responses to environmental change and feedbacks to climate. In J. Houghton & e. al. (Eds.) *Climate Change 1995. Intergovernmental Panel on Climate Change* (pp. 487-516). Cambridge: Cambridge University Press..

Dorman, C. E., Rogers, D. P., Nuss, W. & Thompson, W. T. (1999). Adjustment of the summer marine boundary layer around Point Sur, California. *Monthly Weather Review. 127*, 2143-2159.

Dorman, C. E. & Winant, C. D. (1995). Buoy observations of the atmosphere along the west coast of the United States. *Journal of Geophysical Research, 100*, 16029-16044.

Ebuchi, N., Graber, H. C. & Caruso, J. (2002). Evaluation of wind vectors observed by QuikSCAT/SeaWinds using ocean buoy data. *Journal of Atmospheric and Oceanic Technology, 19*, 2049-2062.

Enríquez, A. G. & Friehe, C. A. (1995). Effects of wind stress and wind stress curl variability on coastal upwelling. *Journal of Physical Oceanography, 25*, 1651-1671.

Franks, P. J. S. (2001). Phytoplankton blooms in a fluctuating environment: the roles of plankton response time scales and grazing. *Journal of Plankton Research*, 23, 1433-1441.

Freilich, M. & Dunbar, R. S. (1999). The accuracy of the NSCAT vector winds: Comparisons with National Data Buoy Center buoys. *Journal of Geophysical Research, 104*, 11231-11246.

Fuenzalida, H. (1971). *Climatologia de Chile.* Santiago: Departamento de Física y Geodesia, Universidad de Chile.

Fuenzalida, R. (1989). Variabilidad temporal de un índice de surgencia para la zona de Iquique (Lat. 20°S). *Invest. Cient. y Tec., Serie: Ciencias del Mar, 1*, 37-47.

Garreaud, R. D., Rutllant, J. & Fuenzalida, H. (2002). Coastal Lows along the Subtropical West Coast of South America: Mean Structure and Evolution. *Monthly Weather Review, 130*, 75-88.

Ghil, M., Allen, M. R., Dettinger, M. D., Ide, K., Kondrashov, D., Mann, M. E., Robertson, A. W., Saunders, A., Tian, Y., Varadi, F. & Yiou, P. (2002). Advanced Spectral Methods for Climatic Time Series. *Reviews of Geophysics, 40*, 1003-doi:10.1029/2000RG00.

Graham, N. E. & White, W. G. (1988). The El Nino Cycle: A Natural Oscillator of the Pacific Ocean-Atmosphere System. *Science, 240*, 1293-1302.

Hare, S. & Mantua, N. J. (2000). Empirical evidence for North Pacific regime shifts in 1977 and 1989. *Progress in Oceanography, 47*, 103-145.

Hayward, L., Baumgartner, T. R., Checkley, D. M., Durazo, R., Castro, G. G., Hyrenbach, K. D., Mantyla, A. W., Mullin, M. M., Murphree, T., Schwing, F. B., Smith, E. P. & Tegner, M. J. (1999). The state of the California Current in 1998-1999: Transition to cool-water conditions. *CalCOFI Reports, 40*, 29-62.

Hellerman, S. & Rosenstein, M. (1983). Normal Monthly Wind Stress Over the World Ocean with Error Estimates. *Journal of Physical Oceanography, 13*, 1093-1104.

Holton, J. & Lindzen, R. S. (1972). An updated theory for the quasi-biennial oscillation of the tropical stratosphere. *Journal of Atmospheric Science, 29*, .

Hormazabal, S., Shaffer, G., Letelier, J. & Ulloa, O. (2001). Local and remote forcing of sea surface temperature in the coastal upwelling system off Chile. *Journal of Geophysical Research, 106*, 16657-16671.

Jollife, I. T. (2002). *Principal Component Analysis*. 2nd New York: Springer-Verlag.

Large, W. G., McWilliams, J. C. & Doney, S. C. (1994). Oceanic vertical mixing: A review and a model with a non-local boundary layer parameterization. *Reviews of Geophysics, 32*, 363-403.

Lasker, R. (1978). The relation between oceanographic conditions and larval anchovy food in the California current: Identification of factors contributing to recruitment fortune. *Rapp. P.-V. Reun. Cons. Int. Mer, 173*, 212-230.

Lau, K.-M. & Weng, H. (1995). Climate signal detection using wavelet transform: How to make a time series sing. *Bulletin of the American Meteorological Society, 76*, 2391-2402.

Lluch-Cota, D. B., Wooster, W. S. & Hare, S. R. (2001). Sea surface temperature variability in coastal areas of the Northeastern Pacific related to the El Niño-Southern Oscillation and the Pacific Decadal Oscillation. *Journal of Geophysical Research, 28*, 2029-2032.

Loeb, V. J. & Rojas, O. (1988). Interannual variation of ichthyoplankton composition and abundance relations off northern Chile, 1964-83. *Fisheries Bulletin Us, 86*, 1-24.

Mann, M. E. & Park, J. (1996). Joint spatio-temporal modes of surface temperature and sea level pressure variability in the Northern Hemisphere during the last century. *Journal of Climate, 9*, 2137-2162.

Mantua, N., Hare, S. R., Zhang, Y., Wallace, J. & Francis, R. C. (1997). A Pacific Interdecadal Climate Oscillation with Impacts on Salmon Production. *Bulletin of the American Meteorological Society, 78*, 1069-1079.

Mantua, N. (2004). Methods for detecting regime shifts in large marine ecosystems: a review with approaches applied to north Pacific data. *Progress In Oceanography, 60*, 165-182.

Marchesiello, P., Mcwilliams, J. C. & Shchepetkin, A. (2003). Equilibrium Structure and Dynamics of the California Current System. *Journal of Physical Oceanography, 33*, 753-783.

Maruyama, T. & Tsuneoka, Y. (1988). Anomalously short duration of the easterly wind phase of the QBO at 50hPa in 1987 & its relationship to an El Nino event. *Journal of the Meteorological Society of Japan. 6*, 629-634.

Maruyama, T. (1997). The quasi-biennial oscillation(QBO) and equatorial waves - a historical review. *Meteorology and Geophysics, 48*, 1-17.

Mass, C. F. & Steenburgh, W. J. (2000). An observational and numerical study of an orographically trapped wind reversal along the west coast of the United States. *Mon. Wea. Rev., 128*, 2363–2396.

McCreary, J. P. (1983). A model of tropical ocean-atmosphere interaction. *Monthly Weather Review, 111*, 330-387.

Menge, B. A., Sanford, E., Daley, B. A., Freidenburg, T. L., Hudson, G. & Lubchenco, J. (2002). An interhemispheric comparison of bottom-up effects on community structure: insights revealed using the comparative-experimental approach. *Ecological Research, 17*, 1-16.

Montecinos, A., Purca, S. & Pizarro, O. (2003). Interannual to interdecadal sea surface temperature variability along the western coast of South America. *Geophysical Research Letters, 30*, -10.1029/2003GL017345.

Montecinos, A. (1991). *Efecto del Fenómeno El Niño en los vientos favorables a la surgencia costera en la zona norte de Chile*. Valparaiso: Departamento de Oceanografia, Universidad Católica de Valparaíso.

Monterey, G. & Levitus, S. (1997). *Seasonal Variability of Mixed Layer Depth for the World Ocean*. Wash., D.C: U.S. Gov. Printing Office.

Murtugudde, R., Beauchamp, J. & Busalacchi, A.J. (1999). *Penetrative Radiation: Observations Requirements*. St. Raphael.

Nakamura, H. & Yamagata, T. (1999). Recent decadal SST variability in the Northwestern Pacific and associated atmospheric anomalies. In A. Navarra (Ed.), *Beyond El Nino: Decadal and Interdecadal Climate Variability* (pp. 49-72). Springer.

Narváez, D. (2000). *Observaciones de Vortices de Mesoescala Frente a la Costa Norte de Chile Utilizando Altimetria Satelital y Datos Hidrograficos*. Valparaíso: Departamento de Oceanografía, Universidad católica de Valparaiso.

Pazan, S. E., White, W. B., Inoue, M. & O'Brien, J. J. (1986). Off-equatorial influence upon Pacific equatorial dynamic height variability during the 1982 – 83 El Nino/Southern Oscillation event. *Journal of Geophysical Research, 91*, 8437-8449.

Peterman, R. M. & Bradford, M. J. (1987). Wind speed and mortality rate of a marine fish, the northern anchovy (Engraulis mordax). *Science, 235*, 354-356.

Peterson, W. T. & Schwing, F. B. (2003). A new climate regime in northeast pacific ecosystems. *Geophysical Research Letters, 30*, 1896-doi:10.1029/2003GL01.

Philander, S.G. (1990). *El Niño, La Niña and the Southern Oscillation*. San Diego: Academic Press.

Pickett, M. H. & Paduan, J. D. (2003). Ekman transport and pumping in the California Current based on the U.S. Navy's high-resolution atmospheric model (COAMPS). *Journal of Geophysical Research, 108*, 3327-doi:10.1029/2003JC00.

Pickett, M., Schwing, F., Collins, C. A., Rosenfeld, L. K., Paduan, J. D. & Wash, C. H. (2004). Improving Wind-Based Upwelling Estimates off the West Coasts of North and South America. *NOAA Technical Memorandum NMFS, January 2004*, .

Pizarro, O., Hormazabal, S., Gonzalez, A. & Yañez, E. (1994). Variabilidad del viento, nivel del mar y temperatura en la costa norte de Chile. *Investigaciones Marinas, 22*, 85-101.

Pond, S. & Pickard, G. L. (1983) Introductory Dynamical Oceanography, 2nd ed., *Pergamon press*, New York, 379.

Power, S., Casey, T., Folland, C., Colman, A. & Mehta, V. (1999). Interdecadal modulation of the impact of ENSO on Australia. *Climate Dynamics, 15*, 319-324.

Press, W.H., Teukolsky, S.A., Vetterling, W.T. & Flannery, B.P. (1992). *Numerical recipes in Fortran 77: the art of scientific computing*. Cambridge: Cambridge University Press.

Pringle, J. M. (2002). Enhancement of wind-driven upwelling and downwelling by alongshore bathymetric variability. *Journal of Physical Oceanography*, 32, 3101– 3112,.

Pringle, J. M. & Riser, K. (2003). Remotely forced nearshore upwelling in Southern California. *Journal of Geophysical Research*, 108, , 3131.

Rasmusson, E. M., Wang, X. & Ropelewski, C. F. (1990). The biennial component of ENSO variability. *Journal of Marine Systems, 1*, 71-96.

Reason, C. J. C. & Jury, M. R. (1990). On the generation and propagation of the southern Africa coastal-low. *Quart. J. Roy. Meteor. Soc., 116*, 1133–1151.

Rieder, K. F., Smith, J. A. & Weller, R. A. (1994). Observed directional characteristics of the wind, wind stress, and surface waves on the open ocean. *Journal of Geophysical Research, 99*, 22589-22596.

Roberts, J. & Roberts, T. D. (1978). Use of the Butterworth Low-Pass filter for Oceanographic Data. *Journal of Geophysical Research, 83*, 5510-5514.

Roemmich, D. & McGowan, J. A. (1995). Climatic warming and the decline of zooplankton in the California Current. *Science, 267*, 1324-1326.

Rudnick, D. L. & Davis, R. E. (2003). Red noise and regime shifts. *Deep Sea Research I, 50*, 691-827.

Rutllant, J., Rosenbluth, B. & Hormazabal, S. (2004). Intraseasonal variability of wind-forced coastal upwelling off central Chile (30°S). *Continental Shelf Research, 24*, 789-804.

Schopf, P. S. & Suarez, M. J. (1988). Vacillations in a coupled ocean-atmosphere model. *Journal of Atmospheric Science, 45*, 549-566.

Schwartzlose, R. A., Alheit, J., Bakun, A., Baumgartner, T. R., Cloete, R., Crawford, R. J., Fletcher, W. J., Green-Ruiz, Y., Hagen, E., Kawasaki, T., Lluch-Belda, D., Lluch-Cota, S. E., MacCall, A. D., Matsuura, Y., Nevarez-Martinez, M. O. & al, e. (1999). Worldwide large-scale fluctuations of sardine and anchovy populations. *South African Journal of Marine Science, 21*, 289-347.

Schwing, F. B. & Mendelssohn, R. (1997). Increased coastal upwelling in the California Current System. *Journal of Geophysical Research, 102*, 3421-3438.

Shaffer, G., Hormazabal, S., Pizarro, O. & Salinas, S. (1999). Seasonal and interannual variability of currents and temperature off central Chile. *Journal of Geophysical Research, 104*(C12), 29951.

Shanks, A. L., Largier, J., Brink, L., Brubaker, J. & Hoff, R. (2000). Evidence for shoreward transport of meroplankton by an upwelling relaxation front. *Limnology and Oceanography, 45*, 230-236.

Shannon, L.V. & O'Toole, M.J. (1999). *Integrated Overview of the Oceanography and Environmental Variability of the Benguela Current Region*. Synthesis and Assessment of Information on The Benguela Current Large Marine Ecosystem (BCLME).

Smith, S. (1988). Coefficients for sea surface wind stress, heat flux, and wind profiles as a function of wind speed and temperature. *Journal of Geophysical Research, 93*, 15467-15472.

Strub, P. T., Mesias, J. M., Montecino, V. & Rutllant, J. (1998). Coastal ocean circulation off western South America. In A. R. Robinson & K. H. Brink (Eds.) *The Sea Vol. 11* (pp. 273-313). New York: John Wiley & Sons, Inc..

Torrence, C. & Compo, G. (1998). A Practical Guide to Wavelet Analysis. *Bulletin of the American Meteorological Society, 79*, 61-78.

Torrence, C. & Webster, P. (1999). Interdecadal Changes in the ENSO–Monsoon System. *Journal of Climate, 12*, 2679-2690.

Tourre, Y. M., Rajagopalan, B., Kushnir, K., Barlow, M. & White, B. W. (2001). Patterns of coherent decadal and interdecadal climate signals in the Pacific Basin during the 20th century. *Geophysical Research Letters, 28*, 2069-10.1029/2000GL012780.

Ulrych, T. J. & Bishop, T. N. (1975). Maximum Entropy Analysis and Autoregressive Decomposition. *Rev. Geophysics and Space Phys., 13*, 183-200.

White, A. W. & Cayan, D. R. (2000). A global El Niño-Southern Oscillation wave in surface temperature and pressure and its interdecadal modulation from 1900 to 1997. *Journal of Geophysical Research, 105*, 11223-11242.

White, W. B., Meyers, G. . J., Donguy, R. & Pazan, S. E. (1985). Short-term climate variability in the thermal structure of the Pacific Ocean during 1979–1982. *Journal of Physical Oceanography, 15*, 1917-1935.

White, W. B., Pazan, S. E., Inoue, M. & O'Brien, J. J. (1986). Off-equatorial influence upon Pacific equatorial dynamic height variability during the 1982–83 El Nino/Southern Oscillation event. *Journal of Geophysical Research, 191*, 8437-8449.

White, W. B., Pazan, S. & Inoue, M. (1987). Hindcast/Forecast of ENSO events based upon the redistribution of observed and model heat content in the western North Pacific, 1984–86. *Journal of Physical Oceanography, 17*, 264-280.

White, W. B., Tourre, Y. M., Barlow, M. & Dettinger, M. (2003). A delayed action oscillator shared by biennial, interannual, and decadal signals in the Pacific Basin. *Journal of Geophysical Research, 108*, 3037-doi:10.1029/2002JC00.

Winant, C. D., Dorman, C. E., Friehe, C. A. & Beardsley, R. C. (1988). The marine layer off northern California: An example of supercritical channel flow. *Journal of Atmospheric Science, 45*, 3588-3605.

Wyrtki, K., Stroup, E., Patzert, W. C., Williams,R. & Quinn, W. (1976). Predicting and Observing El Nino. *Science, 191*, 343-346.

Yañez, E., Barbieri, M. A., Silva, C., Nieto, K. & Espíndola, F. (2001). Climate variability and pelagic fisheries in northern Chile. *Progress in Oceanography, 49*, 581-596.

Zebiak, S. E. & Cane, M. A. (1987). A model El Nino-Southern Oscillation. *Monthly Weather Review, 115*, 2262-2278.

VITA

Jose L. Blanco-Garcia

PERSONAL DATA

Date of Birth: August 3, 1957 Place of Birth: Curico, Chile

EDUCATION

- B.S. Physics - Universidad Católica de Valparaíso (UCV), Chile (1975-1977)
- Professional degree of Oceanographer – UCV, Valparaiso, Chile (1978-1981)
- Ph.D. Candidate. Old Dominion University, Department of Ocean Earth and Atmospheric Sciences, Norfolk, Virginia (2000-2004). Graduated in December 2004. Advisor: Dr. Larry P. Atkinson

EXPERIENCE

1980-1982	Research assistant - Instituto de Fomento Pesquero, Santiago, Chile
1983-1986	Principal Investigator - Instituto de Fomento Pesquero, Santiago, Chile
1987-1991	Logistics and Project Management - Instituto Antartico Chileno, Chile
1991-2000	Principal Investigator - Instituto de Fomento Pesquero, Valparaíso, Chile
2000-2004	Research Assistant - Old Dominion University - CCPO, Norfolk, VA, USA

INDEXED PUBLICATIONS (last four years)

2001 Blanco, J. L; Thomas, A.; Carr, M. E. & Strub, P. T. (2001) Seasonal Climatology of Hydrographic Conditions in the Upwelling Region off Northern Chile. *Journal of Geophysical Research, 106* (C6), 11,451-11,467.

2001 Morales, C., Blanco, J.L., Braun, M., & Silva, N. (2001) Chlorophyll-a distribution and associated oceanographic condition off northern Chile during the summer and autumn 1994 and seasonal comparison for period 1993-1994. *J. Mar. Biol. Ass. UK 81*: 193-206 (2001).

2001 Thomas, A., Blanco, J.L., Carr, M.E., Strub, P.T. & Osses, J. (2001) Oceanographic conditions off Northern Chile during the 1996 La Nina and 1997-1998 El Niño. Part 2: Satellite-measured chlorophyll and temperature patterns. *Journal of Geophysical Research,* 106(C1), 899-915.

2002 Atkinson, L. P., Valle-Levinson, A., Figueroa, D., De Pol-Holz, R., Gallardo, V., Schneider, W., Blanco J. L., & Schmidt, M. (2002) Oceanographic observations in Chilean coastal waters between Valdivia and Concepción. *Journal of Geophysical Research, 107*(C7), 10.1029/2001JC000991

2002 Blanco, J. L; Carr; M. E., Thomas, A. &. Strub, P. T. (2002) Oceanographic conditions off northern Chile during the 1996 La Niña and 1997-1998 El Niño: Part 1: Hydrographic conditions. *Journal of Geophysical Research, 107*(C3), 10.1029/2001JC001002.

2002 Carr, M. E., Strub, P.T., Thomas, A., & Blanco, J.L. (2002) Evolution of 1997-1999 El Nino conditions off the western coast of South America: a remote sensing perspective. *Journal of Geophysical Research, 107*(C12), 3236

2004 Escribano, R., Rosales, S., & Blanco, J. L., (2004) Understanding upwelling circulation off Antofagasta (northern Chile): A three-dimensional numerical-modeling approach. *Continental Shelf Research 24*(1): 37-53.

2004 Valle-Levinson, A. & Blanco, J. L. (2004) Observations of wind influence on Exchange flows in a Strait of the Chilean Inland Sea. *Journal of Marine Research 62*(5)

2004 Atkinson, L. P., Huthnance, J.& Blanco, J. L. (2004) Circulation, Mixing and the Distribution of Re-Mineralized Nutrients. Accepted by *The Sea*.